Response of E. histolytica to L-Cysteine Depletion

We also demonstrated that L-cysteine deprivation repressed glycolysis and energy generation. Upon L-cysteine depletion, pyruvate and other upstream glycolytic intermediates accumulated that appeared to be rerouted toward the associated pathways. For example, the metabolites linked to pyruvate and phosphoenolpyruvate (*i.e.* alanine, malate, and fumarate), 3-phosphoglycerate (*i.e.* O-phosphoserine), and dihydroxyacetone-phosphate (*i.e.* Gly 3-P) increased in response to L-cysteine depletion. In contrast, the level of acetyl-CoA, ethanol, and the major nucleotide triphosphates significantly decreased. In *E. histolytica*, pyruvate is utilized by pyruvate:ferredoxin oxidoreductase, a highly oxygen-sensitive iron-sulfur cluster-containing protein (56). Our data are consistent with the premise that L-cysteine depletion-mediated oxidative stress inactivates pyruvate:ferredoxin oxidoreductase and other redox-sensitive enzymes, which results in the overall reduction in the glycolytic flux and the accumulation of upstream glycolytic intermediates. It has been shown in *E. histolytica* that under oxidative or nitrosative stress, pyruvate, glucose 6-phosphate, and fructose 6-phosphate accumulate, whereas ethanol and ATP decrease (33, 56). Unlike nitrosative stress, L-cysteine depletion for 48 h did not induce apoptosis (data not shown), and the decrease in ATP content appears to be primarily a result of the reduced glycolytic flux. Whole genome microarray analysis has revealed that L-cysteine depletion does not affect the expression of most of the genes involved in energy metabolism, with the exception of phosphoglycerate mutase and malate dehydrogenase, which were slightly down-regulated by 1.6- and 2.1-fold, respectively.[7] Down-regulation of these two genes may also contribute, at least in part, to the overall reduction in the glycolytic flux.

Discovery of Isopropanolamine and PtdIspn Synthesis upon L-Cysteine Deprivation—We have demonstrated for the first time that the Kennedy pathway, the major pathway for phospholipid biosynthesis, is regulated by the level of L-cysteine in *E. histolytica*. L-Cysteine deprivation resulted in the accumulation of an unusual phospholipid, PtdIspn, and also affected the composition and ratio of the major phospholipids. Under L-cysteine-depleted conditions, the synthesis of Ispn, Ispn-P, Etn-P, and Cho-P was elevated, PtdEtn synthesis was down-regulated, and the levels of Etn, Cho, PtdCho, phosphatidylserine, phosphatidylinositol, and phosphatidic acid were unaffected (Fig. 4).

Based on the findings related to phospholipid biosynthesis, we propose the following scheme for the involvement of L-cysteine. When *E. histolytica* is cultured under L-cysteine-depleted conditions, Ispn synthesis is increased. Ispn-P, formed from Ispn and ATP in a reaction catalyzed by Etn/Cho kinase (EHI_148580 (EAL52090.1); EHI_152340 (EAL51511.1)), then competes with Etn-P for Etn-P cytidyltransferase (EHI_095120 (EAL44415.1); EHI_140590 (EAL48799.1)), which appears to be the rate-limiting enzyme for the production of CDP-Ispn. This competition leads to an accumulation of Etn-P and a decrease in PtdEtn. The fact that PtdCho level was not affected by either L-cysteine depletion or Ispn supplementation, whereas Cho-P level increased upon L-cysteine depletion (Fig. 4*A*), suggests that Ispn-P does not compete with Cho-P for Etn-P/Cho-P cytidyltransferase. This observation also indicates that the increase in Cho-P is a consequence of increased production from accumulated Etn-P by SAM-dependent methylation, which may also contribute to the decrement in the SAM level. Alternatively, Ispn-P may compete with Cho-P for Etn-P/Cho-P cytidyltransferase, but the contribution of *de novo* synthesized PtdCho is negligible compared with the PtdCho incorporated from the culture milieu (Fig. 4).

Significance of PtdIspn Production upon L-Cysteine Deprivation—One of the consequences of the L-cysteine-dependent increase in Ispn synthesis is the concomitant increment in Etn-P, which is a known scavenger of free radicals (57). However, the increment of PtdIspn by L-cysteine depletion is not associated with either oxidative stress or changes in the redox status, because D-cysteine did not alleviate the PtdIspn synthesis, and paraquat/air treatment did not increase PtdIspn synthesis.

Similar to PtdEtn, phospahtidyl-propanolamine, an analog of PtdIspn, is a nonbilayer or hexagonal phase-forming phospholipid; however, it is not known whether PtdIspn is also similar to PtdEtn and phospahtidylpropanolamine in its nonbilayer or hexagonal phase-forming nature (58). Hexagonal phase-forming phospholipids have been proposed to be important for membrane fluidity, protein translocation, and membrane fusion events (59, 60). In PtdEtn methylation-defective mutants of *Saccharomyces cerevisiae*, supplementation of the culture medium with propanolamine leads to phosphatidylpropanolamine production and thus presumably compensates for the role of PtdCho and its *N*-methylated phospholipid precursors (58). However, mitochondrial PtdEtn cannot be completely replaced by phosphatidylpropanolamine, suggesting that PtdEtn is essential for the structure and function of mitochondrial membranes (58). It has been shown that changes in the PtdCho/PtdEtn ratio affect membrane integrity of large unilamellar vesicles in mouse hepatocytes, and this ratio is inversely correlated with leakage across the membrane (61). Because L-cysteine depletion also increases the PtdCho/PtdEtn ratio, it is conceivable that this changes membrane integrity and fluidity and affects protein translocation across the plasma membrane. In addition, because PtdEtn also plays various metabolic roles in cells, a decrease in PtdEtn level may also affect other cellular processes, including the synthesis of GPI anchors and protein modification.

To date, this is the first report to show that PtdIspn synthesis is increased by changes in environmental conditions. PtdIspn and phosphatidylpropanolamine have been identified in various organisms, including yeast, protozoa, and animals, and are considered to be unnatural phospholipids synthesized only under conditions where Ispn or propanolamine are supplied in the culture medium (58, 62) or administered intraperitoneally (63). Recently, PtdIspn has been shown to be naturally synthesized in BHK cells through the decarboxylation of the rare phospholipid phosphatidylthreonine (64).

[7] A. Husain, D. Sato, G. Jeelani, M. Suematsu, T. Soga, and T. Nozaki, unpublished data.

In conclusion, we have demonstrated that L-cysteine regulates various metabolic pathways in *E. histolytica* and thus affects the concentrations of the amino acids, phospholipids, and intermediary metabolites involved in central energy metabolism. Further investigation on the physiological role and fate of SMC and PtdIspn will help to better understand sulfur-containing amino acid metabolism, which is considered an attractive drug target for the development of new chemotherapeutics against this pathogen (18, 65). Future research is also needed to understand the function of PtdIspn in the plasma membrane and membrane-bound organelles and in the regulation of phospholipid metabolism.

Acknowledgments—We thank Takako Hishiki (Keio University) for the initial acquisition and analysis of CE-MS data and helpful discussions, Masahiro Sugimoto and Akiyoshi Hirayama (Keio University) for the use of CE-MS data analysis software (MasterHands), and all of the members of our laboratory for technical assistance and valuable discussions.

REFERENCES

1. Beinert, H., Holm, R. H., and Münck, E. (1997) *Science* **277,** 653–659
2. Stanley, S. L., Jr. (2003) *Lancet* **361,** 1025–1034
3. Weinbach, E. C., and Diamond, L. S. (1974) *Exp. Parasitol.* **35,** 232–243
4. Mehlotra, R. K. (1996) *Crit. Rev. Microbiol.* **22,** 295–314
5. Nozaki, T., Asai, T., Kobayashi, S., Ikegami, F., Noji, M., Saito, K., and Takeuchi, T. (1998) *Mol. Biochem. Parasitol.* **97,** 33–44
6. Clark, C. G., Alsmark, U. C., Tazreiter, M., Saito-Nakano, Y., Ali, V., Marion, S., Weber, C., Mukherjee, C., Bruchhaus, I., Tannich, E., Leippe, M., Sicheritz-Ponten, T., Foster, P. G., Samuelson, J., Noël, C. J., Hirt, R. P., Embley, T. M., Gilchrist, C. A., Mann, B. J., Singh, U., Ackers, J. P., Bhattacharya, S., Bhattacharya, A., Lohia, A., Guillén, N., Duchêne, M., Nozaki, T., and Hall, N. (2007) *Adv. Parasitol.* **65,** 51–190
7. Nozaki, T., Asai, T., Sanchez, L. B., Kobayashi, S., Nakazawa, M., and Takeuchi, T. (1999) *J. Biol. Chem.* **274,** 32445–32452
8. Nozaki, T., Ali, V., and Tokoro, M. (2005) *Adv. Parasitol.* **60,** 1–99
9. Hussain, S., Ali, V., Jeelani, G., and Nozaki, T. (2009) *Mol. Biochem. Parasitol.* **163,** 39–47
10. Loftus, B., Anderson, I., Davies, R., Alsmark, U. C., Samuelson, J., Amedeo, P., Roncaglia, P., Berriman, M., Hirt, R. P., Mann, B. J., Nozaki, T., Suh, B., Pop, M., Duchene, M., Ackers, J., Tannich, E., Leippe, M., Hofer, M., Bruchhaus, I., Willhoeft, U., Bhattacharya, A., Chillingworth, T., Churcher, C., Hance, Z., Harris, B., Harris, D., Jagels, K., Moule, S., Mungall, K., Ormond, D., Squares, R., Whitehead, S., Quail, M. A., Rabbinowitsch, E., Norbertczak, H., Price, C., Wang, Z., Guillén, N., Gilchrist, C., Stroup, S. E., Bhattacharya, S., Lohia, A., Foster, P. G., Sicheritz-Ponten, T., Weber, C., Singh, U., Mukherjee, C., El-Sayed, N. M., Petri, W. A., Jr., Clark, C. G., Embley, T. M., Barrell, B., Fraser, C. M., and Hall, N. (2005) *Nature* **433,** 865–868
11. Tokoro, M., Asai, T., Kobayashi, S., Takeuchi, T., and Nozaki, T. (2003) *J. Biol. Chem.* **278,** 42717–42727
12. Sato, D., Yamagata, W., Harada, S., and Nozaki, T. (2008) *FEBS J.* **275,** 548–560
13. Fahey, R. C., Newton, G. L., Arrick, B., Overdank-Bogart, T., and Aley, S. B. (1984) *Science* **224,** 70–72
14. Gillin, F. D., and Diamond, L. S. (1980) *J. Protozool.* **27,** 474–478
15. Gillin, F. D., and Diamond, L. S. (1981) *Exp. Parasitol.* **52,** 9–17
16. Gillin, F. D., and Diamond, L. S. (1981) *Exp. Parasitol.* **51,** 382–391
17. Jeelani, G., Husain, A., Sato, D., Ali, V., Suematsu, M., Soga, T., and Nozaki, T. (2010) *J. Biol. Chem.* **285,** 26889–26899
18. Ali, V., and Nozaki, T. (2007) *Clin. Microbiol. Rev.* **20,** 164–187
19. Soga, T., Baran, R., Suematsu, M., Ueno, Y., Ikeda, S., Sakurakawa, T., Kakazu, Y., Ishikawa, T., Robert, M., Nishioka, T., and Tomita, M. (2006) *J. Biol. Chem.* **281,** 16768–16776
20. Sato, S., Soga, T., Nishioka, T., and Tomita, M. (2004) *Plant J.* **40,** 151–163
21. Soga, T., Ohashi, Y., Ueno, Y., Naraoka, H., Tomita, M., and Nishioka, T. (2003) *J. Proteome Res.* **2,** 488–494
22. Diamond, L. S., Harlow, D. R., and Cunnick, C. C. (1978) *Trans. R. Soc. Trop. Med. Hyg.* **72,** 431–432
23. Clark, C. G., and Diamond, L. S. (2002) *Clin. Microbiol. Rev.* **15,** 329–341
24. Ohashi, Y., Hirayama, A., Ishikawa, T., Nakamura, S., Shimizu, K., Ueno, Y., Tomita, M., and Soga, T. (2008) *Mol. Biosyst.* **4,** 135–147
25. Soga, T., and Heiger, D. N. (2000) *Anal. Chem.* **72,** 1236–1241
26. Soga, T., Ueno, Y., Naraoka, H., Ohashi, Y., Tomita, M., and Nishioka, T. (2002) *Anal. Chem.* **74,** 2233–2239
27. Soga, T., Igarashi, K., Ito, C., Mizobuchi, K., Zimmermann, H. P., and Tomita, M. (2009) *Anal. Chem.* **81,** 6165–6174
28. Sugimoto, M., Wong, D. T., Hirayama, A., Soga, T., and Tomita, M. (2010) *Metabolomics* **6,** 78–95
29. Smith, C. A., Want, E. J., O'Maille, G., Abagyan, R., and Siuzdak, G. (2006) *Anal. Chem.* **78,** 779–787
30. Baran, R., Kochi, H., Saito, N., Suematsu, M., Soga, T., Nishioka, T., Robert, M., and Tomita, M. (2006) *BMC Bioinformatics* **7,** 530
31. Bai, J., Rodriguez, A. M., Melendez, J. A., and Cederbaum, A. I. (1999) *J. Biol. Chem.* **274,** 26217–26224
32. Aceti, D. J., and Ferry, J. G. (1988) *J. Biol. Chem.* **263,** 15444–15448
33. Ramos-Martínez, E., Olivos-García, A., Saavedra, E., Nequiz, M., Sánchez, E. C., Tello, E., El-Hafidi, M., Saralegui, A., Pineda, E., Delgado, J., Montfort, I., and Pérez-Tamayo, R. (2009) *Int. J. Parasitol.* **39,** 693–702
34. Bligh, E. G., and Dyer, W. J. (1959) *Can. J. Biochem. Physiol.* **37,** 911–917
35. Zhou, X., and Arthur, G. (1992) *J. Lipid Res.* **33,** 1233–1236
36. Rébeillé, F., Jabrin, S., Bligny, R., Loizeau, K., Gambonnet, B., Van Wilder, V., Douce, R., and Ravanel, S. (2006) *Proc. Natl. Acad. Sci. U.S.A.* **103,** 15687–15692
37. Giovanelli, J., Mudd, S. H., and Datko, A. H. (1980) in *The Biochemistry of Plants* (Miflin B. J., eds.), Vol. 5, pp. 453–487, Academic Press, New York
38. Zuo, X., and Coombs, G. H. (1995) *FEMS Microbiol. Lett.* **130,** 253–258
39. Husain, A., Jeelani, G., Sato, D., Ali, V., and Nozaki, T. (2010) *Mol. Biochem. Parasitol.* **170,** 100–104
40. Anderson, I. J., and Loftus, B. J. (2005) *Exp. Parasitol.* **110,** 173–177
41. Kelley, J. J., and Dekker, E. E. (1984) *J. Biol. Chem.* **259,** 2124–2129
42. Green, M. L., and Elliott, W. H. (1964) *Biochem. J.* **92,** 537–549
43. Ray, M., and Ray, S. (1987) *J. Biol. Chem.* **262,** 5974–5977
44. Inoue, Y., and Kimura, A. (1995) *Adv. Microb. Physiol.* **37,** 177–227
45. Westrop, G. D., Goodall, G., Mottram, J. C., and Coombs, G. H. (2006) *J. Biol. Chem.* **281,** 25062–25075
46. Ariyanayagam, M. R., and Fairlamb, A. H. (1999) *Mol. Biochem. Parasitol.* **103,** 61–69
47. Wirtz, M., Birke, H., Heeg, C., Mueller, C., Hosp, F., Throm, C., Koenig, S., Feldman-Salit, A., Rippe, K., Petersen, G., Wade, R. C., Rybin, V., Scheffzek, K., and Hell, R. (2010) *J. Biol. Chem.* **285,** 32810–32817
48. Kredich, N. M. (1992) *Mol. Microbiol.* **6,** 2747–2753
49. Horner, W. H., and Kuchinskas, E. J. (1959) *J. Biol. Chem.* **234,** 2935–2937
50. Ronald, C. D., and John, F. T. (1971) *Phytochemistry* **10,** 1745–1750
51. Mae, T., and Ohira, K. (1976) *Plant Cell Physiol.* **17,** 459–465
52. Mae, T., Ohira, K., and Fujiwara, A. (1971) *Plant Cell Physiol.* **12,** 881–887
53. Wiebers, J. L., and Garner, H. R. (1964) *J. Bacteriol.* **88,** 1798–1804
54. Pérez-Mato, I., Castro, C., Ruiz, F. A., Corrales, F. J., and Mato, J. M. (1999) *J. Biol. Chem.* **274,** 17075–17089
55. Kuhlmann, M. K., and Vadgama, J. V.(1991) *J. Biol. Chem.* **266,** 15042–15047
56. Ramos, E., Olivos-García, A., Nequiz, M., Saavedra, E., Tello, E., Saralegui, A., Montfort, I., and Pérez Tamayo, R. (2007) *Exp. Parasitol.* **116,** 257–265
57. Gordon, I. I., Weiss, D., Prachand, S., and Weitzman, S. A. (1991) *Free Radic. Res. Commun.* **15,** 65–71
58. Choi, J. Y., Martin, W. E., Murphy, R. C., and Voelker, D. R. (2004)

J. Biol. Chem. **279,** 42321–42330
59. Yeagle, P. L. (1989) *FASEB J.* **3,** 1833–1842
60. Cullis, P. R., Fenske, D. B., and Hope, M. J. (1996) in *Biochemistry of Lipids, Lipoproteins and Membranes* (Vance, D. E., and Vance, J., eds) Vol. 31, pp. 1–33, Elsevier, Paris
61. Li, Z., Agellon, L. B., Allen, T. M., Umeda, M., Jewell, L., Mason, A., and Vance, D. E. (2006) *Cell Metab.* **3,** 321–331
62. Smith, J. D., and Barrows, L. J. (1988) *Biochem. J.* **254,** 301–302
63. Meyer, W., Wahl, R., and Gercken, G. (1979) *Biochim. Biophys. Acta* **575,** 463–466
64. Heikinheimo, L., and Somerharju, P. (2002) *Traffic* **3,** 367–377
65. Sato, D., Kobayashi, S., Yasui, H., Shibata, N., Toru, T., Yamamoto, M., Tokoro, G., Ali, V., Soga, T., Takeuchi, T., Suematsu, M., and Nozaki, T. (2010) *Int. J. Antimicrob. Agents* **35,** 56–61

THE JOURNAL OF BIOLOGICAL CHEMISTRY VOL. 285, NO. 35, pp. 26889–26899, August 27, 2010

Two Atypical L-Cysteine-regulated NADPH-dependent Oxidoreductases Involved in Redox Maintenance, L-Cystine and Iron Reduction, and Metronidazole Activation in the Enteric Protozoan *Entamoeba histolytica*[*][S]

Received for publication, January 24, 2010, and in revised form, June 28, 2010 Published, JBC Papers in Press, June 30, 2010, DOI 10.1074/jbc.M110.106310

Ghulam Jeelani[‡§1], Afzal Husain[‡], Dan Sato[¶], Vahab Ali[‖], Makoto Suematsu[**], Tomoyoshi Soga[¶], and Tomoyoshi Nozaki[‡1,2]

From the [‡]Department of Parasitology, National Institute of Infectious Diseases, 1-23-1 Toyama, Shinjuku-ku, Tokyo 162-8640, Japan, the [§]Center for Integrated Medical Research, School of Medicine, Keio University, Shinjuku, Tokyo 160-8582, Japan, the [¶]Institute for Advanced Biosciences, Keio University, Tsuruoka, Yamagata 997-0052, Japan, the [‖]Department of Biochemistry, Rajendra Memorial Research Institute of Medical Sciences, Agamkuan, Patna-800007, India, and the [**]Department of Biochemistry and Integrative Medical Biology, School of Medicine, Keio University, Shinjuku, Tokyo 160-8582, Japan

We discovered novel catalytic activities of two atypical NADPH-dependent oxidoreductases (EhNO1/2) from the enteric protozoan parasite *Entamoeba histolytica*. EhNO1/2 were previously annotated as the small subunit of glutamate synthase (glutamine:2-oxoglutarate amidotransferase) based on similarity to authentic bacterial homologs. As *E. histolytica* lacks the large subunit of glutamate synthase, EhNO1/2 were presumed to play an unknown role other than glutamine/glutamate conversion. Transcriptomic and quantitative reverse PCR analyses revealed that supplementation or deprivation of extracellular L-cysteine caused dramatic up- or down-regulation, respectively, of EhNO2, but not EhNO1 expression. Biochemical analysis showed that these FAD- and 2[4Fe-4S]-containing enzymes do not act as glutamate synthases, a conclusion which was supported by phylogenetic analyses. Rather, they catalyze the NADPH-dependent reduction of oxygen to hydrogen peroxide and L-cystine to L-cysteine and also function as ferric and ferredoxin-NADP$^+$ reductases. EhNO1/2 showed notable differences in substrate specificity and catalytic efficiency; EhNO1 had lower K_m and higher k_{cat}/K_m values for ferric ion and ferredoxin than EhNO2, whereas EhNO2 preferred L-cystine as a substrate. In accordance with these properties, only EhNO1 was observed to physically interact with intrinsic ferredoxin. Interestingly, EhNO1/2 also reduced metronidazole, and *E. histolytica* transformants overexpressing either of these proteins were more sensitive to metronidazole, suggesting that EhNO1/2 are targets of this anti-amebic drug. To date, this is the first report to demonstrate that small subunit-like proteins of glutamate synthase could play an important role in redox maintenance, L-cysteine/L-cystine homeostasis, iron reduction, and the activation of metronidazole.

Glutamate synthase (glutamine:2-oxoglutarate amidotransferase, GOGAT[3]) is an iron sulfur flavoprotein that catalyzes the transfer of the amide group of L-glutamine to 2-oxoglutrate to yield L-glutamate and is a key enzyme in the nitrogen assimilation pathway. In eubacteria, this enzyme is dependent on the pyridine nucleotide NAD(P)H for its reducing equivalents and is composed of large 150-kDa (α) and small 50-kDa (β) subunits that together form the active $\alpha\beta$ protomer (1). The structural genes encoding the α and β subunit polypeptides are commonly designated *gltB* and *gltD*, respectively, and lie adjacent on the chromosome with the α subunit preceding the β subunit, except in γ-proteobacteria, where the gene order is reversed. The small subunit of eubacterial glutamate synthase shows sequence similarity to several other protein domains and enzyme subunits (2, 3) and is, therefore, proposed to represent a prototype domain used in many different cellular processes to transfer electrons from NAD(P)H to an acceptor protein or protein domain of unknown function (4). In concord with this view, numerous organisms have been recently identified to possess glutamate synthase β subunit-like genes based on DNA sequence homology (4, 5); however, the organisms often lack a gene encoding the corresponding α subunit, or the β subunit is not present adjacent to the α subunit and is, therefore, transcribed independently (5, 6). To our knowledge, among the organisms lacking a putative GOGAT α subunit, only the GOGAT β subunit from *Thermococcus kodakaraensis* (renamed from *Pyrococcus* sp. KOD1) has been functionally associated with independent GOGAT activity (7).

* This work was supported by Grants-in-aid for Scientific Research 18GS0314, 18050006, and 18073001 (to T. N.) from the Ministry of Education, Culture, Sports, Science, and Technology of Japan, a grant for research on emerging and re-emerging infectious diseases from the Ministry of Health, Labour, and Welfare of Japan (H20-Shinkosaiko-016), and a grant for research to promote the development of anti-AIDS pharmaceuticals from the Japan Health Sciences Foundation (to T. N.).

[S] The on-line version of this article (available at http://www.jbc.org) contains supplemental Figs. S1–S3.

The nucleotide sequence(s) reported in this paper has been submitted to the GenBank™/EBI Data Bank with accession number(s) AB521132 and AB521133.

[1] Supported in part by the Global Center of Excellence Program for Human Metabolomic System Biology of the Ministry of Education Culture, Sports, Science, and Technology.

[2] To whom correspondence should be addressed. Tel.: 81-3-5285-1111 (ext. 2600); Fax.: 81-3-5285-1219; E-mail: nozaki@nih.go.jp.

[3] The abbreviations used are: GOGAT, glutamine:2-oxoglutarate amidotransferase; EhNO, *E. histolytica* NADPH-dependent oxidoreductase; rEhNO, recombinant EhNO; INT, iodonitrotetrazolium; CE, capillary electrophoresis; SoFd, *S. oleracea* ferredoxin; EhFd1, *E. histolytica* ferredoxin.

Entamoeba histolytica, the causative agent of human amebiasis, is an enteric protozoan parasite responsible for amebic colitis and extraintestinal abscesses in approximately 50 million inhabitants of endemic areas (8). As is the case with other microaerophilic parasitic infections, such as giardiasis and trichomoniasis, the 5-nitroimidazole drug metronidazole has been established as the most effective treatment of amebiasis. Because of the high prevalence of these infections (9) and because of its role as a second-line defense against *Helicobacter pylori* infections (10), metronidazole has been included in the list of "essential medicines" by the World Health Organization (11). Metronidazole is a prodrug that requires reduction of the nitro group to generate the cytotoxic nitroradical anion that undergoes further reduction resulting in the generation of nitrosoimidazole (12, 13). This active form can then react with sulfhydryl groups (14) and DNA (15) while being further reduced to an amine via a hydroxylamine intermediate. Here, we report for the first time multiple novel roles of two GOGAT β subunit-like proteins in *E. histolytica*. We demonstrated that they are not associated with glutamate synthase activity but instead exhibit robust reductase activities against L-cystine, ferredoxin, and ferric ion and are also involved in the response to oxidative stress. In addition, we showed that these enzymes can be capable of reducing and activating metronidazole and, thus, are responsible for its observed toxicity against *E. histolytica*. We designated the novel NADPH-dependent oxidoreductases as EhNO1 and -2.

EXPERIMENTAL PROCEDURES

Chemicals and Reagents—L-Cysteine, L-cystine, *trans*-epoxysuccinyl-L-leucylamido-(4-guanidino) butane, cytochrome *c*, iodonitrotetrazolium (INT), and metronidazole were purchased from Sigma. Nickel-nitrilotriacetic acid-agarose was purchased from Merck. All other chemicals of analytical grade were purchased from Wako Pure Chemical (Osaka, Japan) unless otherwise stated.

Microorganisms and Cultivation—Trophozoites of the *E. histolytica* clonal strain HM1:IMSS cl 6 were maintained axenically in Diamond's BI-S-33 medium at 35.5 °C as described previously (16, 17). Trophozoites were harvested in the late logarithmic growth phase for 2–3 days after inoculation of 1/30 to 1/12 of the total culture volume. After the cultures were chilled on ice for 5 min, trophozoites were collected by centrifugation at 500 × *g* for 10 min at 4 °C and washed twice with ice-cold PBS (pH 7.4). *Escherichia coli* BL21 (DE3) strain was purchased from Invitrogen.

Quantitative Real-time PCR—Trophozoites were cultured in BI-S-33 medium supplemented with or without 10 mM L-cysteine (18 or 8 mM final, respectively). After placing the culture on ice for 5 min, the trophozoites were harvested by centrifugation at 500 × *g* for 5 min at 4 °C. Polyadenylated RNA was extracted from ~6×10^6 tropozoites with an mRNA isolation kit (Stratagene, La Jolla, CA) and then treated with deoxyribonuclease I (Invitrogen). cDNA was reverse-transcribed with 4 μg of isolated polyadenylated RNA, the SuperScript III First-Strand Synthesis System, and an oligo$(dT)_{20}$ primer (Invitrogen). PCR was performed with the resulting cDNA as a template and specific oligonucleotide primers using the ABI PRISM 7300 Sequence Detection System (Applied Biosystems, Japan). The primers used were 5′-AGCTGCACCAGTTCCAATTC-3′ and 5′-CAATCCCCAGCTGCATATAA-3′ (EhNO1), 5′-CAGTTCCAATTCCAGGCAGT-3′ and 5′-TTGGTCCTGTAACACAATCTCCT-3′ (EhNO2), and 5′-GATCCAACATATCCTAAAACAACA-3′ and 5′-TCAATTATTTTCTGACCCGTCTTC-3′ (RNA polymerase II 15-kDa subunit, GenBank™ accession number XM_643999). The parameters for PCR were as follows: an initial step of denaturation at 95 °C for 9 min followed by 40 cycles of denaturation at 94 °C for 30 s, annealing at 50 °C for 30 s, and extension at 65 °C for 1 min and a final step at 95 °C for 9 s, 60 °C for 9 s, and 95 °C for 9 s was used to remove primer dimers.

Amino Acid Comparison and Phylogenetic Analysis—Amino acid sequences of the GOGAT β subunit and β subunit-like proteins from 40 other organisms were obtained from the DDBJ/EBI/GenBank™ data base using BLASTP searches with the novel amebic NADPH-dependent oxidoreductases (EhNO1 and EhNO2) described in this paper as queries. Sequence alignments of these proteins were generated using the ClustalW program (18). The alignments obtained by ClustalW were inspected and manually corrected using the Genedoc program (19). After the removal of all gaps, 326 unambiguously aligned residues were selected for phylogenetic analyses. The neighbor-joining and maximum parsimony methods were used to construct a final phylogenetic tree for 32 sequences using the MEGA4.1 program (20). The branch lengths and bootstrap values of 1000 replicates (in percentage) in these trees were obtained from the neighbor-joining analysis.

Construction of Plasmids—Standard techniques were used for cloning and plasmid construction, as previously described (21). Genes encoding EhNO1 and EhNO2 were cloned to produce a fusion protein containing a histidine tag (provided by the vector) at the amino terminus. The cDNA corresponding to the open reading frames of EhNO1 and EhNO2 was amplified by PCR using an *E. histolytica* cDNA library (22) as a template and oligonucleotide primers. The sense and antisense oligonucleotide primers used to amplify EhNO1 and EhNO2 were 5′-CTTATAA**GGATCC**ATGAAGAGTTTCAACATTA-3′ and 5′-ATA**GTCGAC**TTAATCTTGTTCCATTGGG-3′ (EhNO1) and 5′-CTTATAA**GGATCC**ATGGCTGCTAATTATAATA-3′ and 5′-ATA**GTCGAC**TTATTCTTCATTTTTTTTACCC-3′ (EhNO2) (bold letters indicate BamHI and SalI restriction sites). PCR was performed with Platinum *Pfx* DNA polymerase (Invitrogen) and the following parameters: an initial incubation at 94 °C for 2 min followed by 30 cycles of denaturation at 94 °C for 15 s, annealing at 45 °C for 30 s, and elongation at 68 °C for 2 min and a final extension at 68 °C for 10 min. The PCR fragments were digested with BamHI and SalI, subjected to gel electrophoresis, excised, purified with the Gene clean kit II (BIO 101, Vista, CA), and then ligated into BamHI- and SalI-digested pCOLD I (Takara Bio, Otsu, Japan) in the identical orientation as the T7 promoter to generate pCOLD1-EhNO1 and pCOLD1-EhNO2. The nucleotide sequences of the cloned EhNO1 and EhNO2 genes were verified by sequencing to be identical to the putative protein coding

regions of XP_656997 and XP_653573, respectively, in *E. histolytica*.

Bacterial Expression and Purification of Recombinant EhNO (rEhNO)—The pCOLD1-EhNO1 and pCOLD1-EhNO2 expression constructs were introduced into competent *E. coli* BL21 (DE3) cells by heat shock at 42 °C for 30 s, and the resulting transformants were grown at 37 °C in 100 ml of Luria Bertani medium in the presence of 50 μg/ml ampicillin. The overnight culture was then used to inoculate 500 ml of fresh medium, which was further cultured at 37 °C with shaking at 180 rpm. When the A_{600} reached 0.6, 1 mM isopropyl β-D-thiogalactopyranoside was added to induce protein expression, and cultivation was continued for 24 h at 15 °C. The *E. coli* cells were then harvested by centrifugation at 4050 × *g* for 20 min at 4 °C, and the resulting cell pellet was washed with PBS (pH 7.4) and re-suspended in 20 ml of lysis buffer (50 mM Tris-HCl (pH 8.0), 300 mM NaCl, and 10 mM imidazole) containing 0.1% Triton X-100 (v/v), 100 μg/ml lysozyme, and 1 mM phenylmethylsulfonyl fluoride. After a 30-min incubation at room temperature, the cells were sonicated on ice and centrifuged at 25,000 × *g* for 15 min at 4 °C. The supernatant was mixed with 1.2 ml of a 50% nickel-nitrilotriacetic acid His-bind slurry (Qiagen, Tokyo, Japan) and incubated for 1 h at 4 °C with gentle shaking. The rEhNO-bound resin was washed three times with buffer A (50 mM Tris-HCl (pH 8.0), 300 mM NaCl, and 0.1% Triton X-100, v/v) containing 10–50 mM imidazole, and bound proteins were then eluted with buffer A containing 100–300 mM imidazole. After the integrity and purity of the rEhNO proteins were confirmed by 12% SDS-PAGE analysis and Coomassie Brilliant Blue staining, they were extensively dialyzed twice against a 300-fold volume of 50 mM Tris-HCl, 150 mM NaCl, pH 8.0, containing 10% glycerol (v/v) and the Complete Mini Protease Inhibitor Mixture (Roche Applied Science) for 18 h at 4 °C. The concentrations of the dialyzed proteins were spectrophotometrically determined by the Bradford method using bovine serum albumin as a standard as previously described (23). The rEhNO proteins were stored at −80 °C in 20% glycerol in small aliquots until needed.

Analysis of Prosthetic Groups—UV-visible absorption spectra of rEhNO1 (400 μg) and rEhNO2 (200 μg) were measured under both non-reducing and sodium dithionite-reducing conditions. The purified recombinant proteins were reduced with a 10-fold molar excess of sodium dithionite in 200 μl. Flavin was liberated from the recombinant enzymes by boiling samples for 10 min and then separated from proteins by centrifugation at 14,000 × *g* for 10 min. To determine whether FAD or FMN formed a prosthetic group, the fluorescence with excitation and emission wavelengths of 450 and 535 nm, respectively, was measured at pH 2.6 and 7.7 according to the method of Faeder and Siegel (24) using a fluorescence spectrophotometer (model F-2500; Hitachi).

Iron Assay—The iron content of EhNOs was determined by the *O*-phenanthroline method as previously described (25). Briefly, 60 μl samples of rEhNO1 and rEhNO2 were mixed with 4 μl of concentrated HCl and then diluted with distilled water to 0.2 ml. After the resulting mixtures were heated to 80 °C for 10 min and cooled to room temperature, they were then mixed with 0.6 ml of water, 40 μl of 10% hydroxylamine hydrochloride, and 0.2 ml of 0.1% *O*-phenanthroline and further incubated at room temperature for 30 min. The absorbances at 512 nm (A_{512}) were then measured, and the iron concentrations were determined by comparison to a standard curve generated with 0–100 μM ferrous sulfate.

Enzyme Assays—Glutamate synthase activity was assayed spectrophotometrically by measuring the rate of NADPH or NADH oxidation at 340 nm with slight modifications of the procedure described by Jongsareejit *et al.* (7). The 200-μl assay mixture contained 20 mM potassium phosphate buffer, pH 7.5, 5 mM concentrations each of L-glutamine and 2-oxoglutarate, 0.4 mM cofactor (NADPH or NADH), and varying concentrations of rEhNO proteins. The reaction was initiated by the addition of cofactor and was performed at 37 °C. To test for ammonia-dependent activity, glutamine was replaced with 100 mM NH_4Cl.

Oxidoreductase Activity—The NADPH-dependent reduction of menadione was monitored in a coupling assay under aerobic conditions. The rate of reduction of cytochrome *c* by menadione was monitored by the absorbance at 550 nm (ϵ_{550} = 21.1 mM^{-1} cm^{-1}). Measurements were made in 50 mM Tris-HCl (pH 7.5), 200 μM NADPH, 1 μM menadione, and 30 μM cytochrome *c*. The reactions were initiated by the addition of 2 μg of rEhNO1/2.

For the other electron acceptors tested, a standard mixture containing 0.1 mM NADPH, 50 mM Tris-HCl (pH 7.5), and either 0.5 mM INT, 1 mM potassium ferricyanide, or 10 mM paraquat was used. The reactions were initiated by the addition of 2 μg of rEhNO1/2 enzyme, and the reduction of the acceptors was monitored spectrophotometrically at 490 nm for INT (ϵ = 18.5 mM^{-1} cm^{-1}), 410 nm for potassium ferricyanide (ϵ = 1 mM^{-1} cm^{-1}), and 340 nm for paraquat (NADPH oxidation, ϵ = 6.22 mM^{-1} cm^{-1}). One unit of enzyme activity was defined as the formation of 1 μmol of product/min/mg of protein.

Metronidazole reduction activity was determined by measuring the oxidation of NADPH at 340 nm (ϵ_{340} = 6.22 mM^{-1} cm^{-1}) or the reduction of metronidazole at 360 nm (ϵ_{360} = 9.2 mM^{-1} cm^{-1}), as described by Chen and Blanchard (26). Assays were conducted at room temperature under strict anaerobic conditions. The reactions were initiated by the addition of 2 μg of rEhNO protein to a mixture comprising 50 mM Tris-HCl (pH 8.0), 0.5 mM metronidazole, and 0.2 mM NADPH.

The cystine reductase activity was calculated as μmol of NADPH oxidized per min at 340 nm. The assay mixture contained 0.1 M potassium phosphate (pH 7.5), 2 mM EDTA, 0.05–0.2 mM NADPH, and 0.1–5 mM L-cystine. Approximately 2 μg of rEhNO1/2 was added to initiate the reaction, and the change in absorbance at 340 nm was monitored. The effects of sulfydryl-dependent inhibitors were examined by preincubation of 2 μg of rEhNO1 and rEhNO2 with 0.1–5 mM *N*-ethylmaleimide for 10 min before the various assays. All sample reactions were performed in triplicate at a minimum.

NAD(P)H:flavin oxidoreductase activity was assayed by measuring the initial rate of NAD(P)H oxidation at 340 nm (ϵ = 6.22 $mM^{-1}cm^{-1}$) at 25 °C as described by Lo and Reeves (27). One unit of NAD(P)H:flavin oxidoreductase activity was defined as the amount of enzyme that catalyzed the oxidation of 1 μmol of NAD(P)H/min.

Ferric reductase activity was determined by measuring the difference of NAD(P)H consumption at 340 nm in the presence and absence of Fe(III) ammonium citrate. Reaction mixtures containing 0.2 mM NADPH, 100 mM Tris-HCl (pH 7.5), 0.005–1 mM ferric ammonium citrate, and 2 μg of rEhNO1 and -2 were used for the assays.

Ferredoxin-$NADP^+$ reductase activity was determined by measuring ferredoxin-dependent reduction of cytochrome *c* (28). Activity was measured by monitoring cytochrome *c* reduction at 550 nm ($\epsilon = 21.1\ mM^{-1}\ cm^{-1}$) in a reaction mixture containing 0.1 mM NADPH, 0.01–0.5 μM ferredoxin, 10 μM cytochrome *c*, and 50 mM Tris-HCl buffer (pH 7.5). The reactions were initiated by the addition of 1 μg of rEhNO1 and -2.

Determination of H_2O_2 Formation—The ferrithiocyanate method (29) was used to measure H_2O_2 formation at various time points (1–30 min) during the NADPH:favin oxidoreductase reaction. After the reactions were terminated by the addition of 0.125 volumes of 50% trichloroacetic acid, the samples were centrifuged at 12,000 × *g*, and 0.2 volumes of 10 mM ferrous ammonium sulfate and 0.1 volumes of 2.5 M potassium thiocyanate were then added. In the presence of H_2O_2, Fe^{2+} is oxidized, resulting in a colored thiocyanate-Fe^{3+} complex that can be measured by its absorption at 480 nm. The quantity of H_2O_2 formed was determined by comparison of the A_{480} values to standard curves generated using known amounts of H_2O_2.

Metabolite Extraction—Approximately 1.5×10^6 *E. histolytica* cells were harvested after 48 h of cultivation and washed twice with 5% mannitol. The cells were then resuspended in 1.6 ml of methanol containing 20 μM concentrations of the internal standard methionine sulfone acid and mixed with 1.6 ml of chloroform and 640 μl of deionized water. After vortexing, the mixture was centrifuged at 4600 × *g* at 4 °C for 5 min, and the aqueous layer (1.6 ml) was filtrated using an Amicon Ultrafree-MC ultrafilter (Corporation, Billerica, MA) by centrifugation at 9100 × *g* at 4 °C for ~2 h. The filtrate was dried and preserved at −80 °C until mass spectrometric analysis.

Instrumentation and Capillary Electrophoresis (CE)-Time of Flight Mass Spectrometry (TOFMS) Conditions—CE-TOFMS was carried out using an Agilent CE Capillary Electrophoresis System equipped with an Agilent 6210 Time-of-Flight mass spectrometer, Agilent 1100 isocratic HPLC pump, Agilent G1603A CE-MS adapter kit, and Agilent G1607A CE-ESI-MS sprayer kit (Agilent Technologies, Waldbronn, Germany). The system was controlled by Agilent G2201AA ChemStation software for CE. Data acquisition was performed by Analyst QS Build: 7222 software for Agilent TOF (Applied Biosystems/MDS Sciex, Ontario, Canada). Instrumental conditions for the separation and detection of metabolites were as follows. The metabolites were separated on a fused silica capillary (50 μm × 100 cm) using 1 M formic acid as the electrolyte, and the applied voltage was set at +30 kV. A solution of 50% (v/v) methanol-water was delivered as the sheath liquid at 10 μl/min (30, 31). Electrospray ionization-TOFMS was conducted in the positive ion mode (4000 V). The pressure of dry nitrogen gas was maintained at 10 p.s.i. Exact mass data were acquired over a 50–1000 *m/z* range (32, 33). Before analysis, the sample was dissolved in 20 μl of deionized water containing 200 μM concentrations of the internal standard 3-aminopyrrolidine.

Generation of E. histolytica Transformants Overexpressing EhNO—The protein coding regions of EhNO1 and EhNO2 were amplified by PCR from cDNA using sense and antisense oligonucleotides containing appropriate restriction sites at the 5′ end. The sense and antisense oligonucleotide primers used for EhNO1 and EhNO2 were 5′-CTA**CCCGGG**ATGAAGAG-TTTCAACATTACA-3′ and 5′-CAA**CTCGAG**TTAATCTT-GTTCCATTGGGGT-3′ (EhNO1) and 5′-CTA**CCCGGG**AT-GGCTGCTAATTATAATAGA-3′ and 5′-CAA**CTCGAG**TT-ATTCATTTTTTTTACC-3′ (EhNO2) (bold letters indicate restriction sites). The PCR-amplified DNA fragments were digested with SmaI and XhoI and ligated into SmaI and XhoI sites of the expression vector pKT-MR (34) to produce pKT-MR-NO1 and pKT-MR-NO2. Wild-type trophozoites were transformed with pKT-MR by liposome-mediated transfection as previously described (35). Transformants were initially selected in the presence of 3 μg/ml Geneticin (Invitrogen), which was then gradually increased to 6–20 μg/ml during the subsequent 2 weeks before subjecting the transformants to analyses.

Assay for Metronidazole Sensitivity of E. histolytica Trophozoites—To determine sensitivity to metronidazole, *E. histolytica* transfectants harboring pKT-MR-NO1, pKT-MR-NO2, or pKT-MR (control) were cultured at 37 °C in BI-S-33 medium containing 20 μg/ml Geneticin. For the assay, varying concentrations (0–16 μM) of metronidazole were added to samples containing an initial density of 10^4 cells/ml. After 48 h, the number of viable cells was counted on a hemocytometer using trypan blue to identify dead cells. The assays were performed five times in duplicate.

In Vitro Interaction of EhNO1/2 with Ferredoxin—Protein cross-linking was performed as described previously (36). Briefly, EhNO1/2 and ferredoxin (4 and 20 μM, respectively) were cross-linked by treatment with 5 mM *N*-ethyl-3-(3-dimethylaminopropyl)carbodiimide in 25 mM sodium phosphate, pH 7.5. The resulting complexes were analyzed by SDS-PAGE and Western blotting using anti-His antibody.

Immunoblot Analysis—Cell lysates and culture supernatants were separated on 12% (w/v) SDS-PAGE gels and subsequently electro-transferred onto nitrocellulose membranes (Hybond-C Extra; Amersham Biosciences) as previously described (37). Nonspecific binding was blocked by incubating the membranes for 1.5 h at room temperature in 5% nonfat dried milk in TBST (50 mM Tris-HCl (pH 8.0), 150 mM NaCl, and 0.05% Tween 20). The blots were then reacted with primary antibodies specific for EhNO1 and EhNO2 and mannose 6-phosphate receptor 1 (38) and cysteine synthase 1 (22) as controls for the membrane and cytosolic fractions, respectively, at dilutions of 1:500 to 1:100. Antisera against purified rEhNO1 and rEhNO2 were raised in rabbits commercially (Operon, Tokyo, Japan). The membranes were washed with TBST and further reacted with horseradish peroxidase-conjugated anti-rabbit or anti-mouse IgG antisera (1:20,000) (Invitrogen) at room temperature for 1.5 h. After further washing with TBST, specific proteins were visualized and measured with a chemiluminescence detection

system (Millipore) using Scion Image software (Scion Corp., Frederick, MD) (39).

RESULTS

Identification of a GOGAT Small β Subunit Gene in E. histolytica upon L-Cysteine Supplementation—Upon analysis of the transcriptome of *E. histolytica* trophozoites cultured in medium supplemented with L-cysteine, a highly up-regulated gene (XM_648481) was previously identified.[4] Although the entire transcriptome data is described elsewhere, we attempted to characterize this gene in detail in the present study. The identified gene and a gene (XM_651905) that appeared to be very closely related in the *E. histolytica* genome data base (40) were predicted to encode proteins showing high similarity to the small β subunit of GOGAT from bacteria. The genes were designated as *E. histolytica* NADPH-dependent oxidoreductase 1 and 2 [EhNO1 (XM_651905) and EhNO2 (XM_648481)] because although the encoded proteins lacked glutamate synthase activity, they showed robust NADPH-dependent oxidoreductase activity (described below). The EhNO1 and EhNO2 genes consisted of 1347- and 1338-bp open reading frames, respectively, which were predicted to encode proteins of 448 and 445 amino acids with predicted molecular masses of 49.3 and 49.0 kDa and isoelectric points of 6.31 and 7.02, respectively.

Features of the Deduced Protein Sequence of EhNOs—The predicted amino acid sequences of the two EhNOs shared 80% mutual identity and demonstrated 20–60% identities to the small β subunit of GOGAT from Archaea, bacteria, animals, and plants. EhNO1 had the highest amino acid identities to the GOGAT β subunit-like proteins of *Chlorobium tepidum* (green sulfur bacteria) and *Methanosarcina mazei* (Archaea) (62 and 59%, respectively), whereas EhNO2 showed 61–62% identities to the small subunit of *Pyrococcus abyssi* GOGAT and the β subunit chain of formate dehydrogenase from *Moorella thermoacetica* (Archaea). Although a multiple alignment of 32 GOGAT and GOGAT-like sequences was generated using ClustalW, the comparisons of representative sequences from *E. coli*, *Clostridium saccharobutylicum*, *Azospirillum brasilense*, and *E. histolytica* were sufficient to highlight the important similarities and differences among GOGAT proteins from these organisms and between the two EhNO isotypes (supplemental Fig. S1).

All of the functional domains characteristic of GOGAT β subunits were conserved between these β subunit-like proteins (supplemental Fig. S1). Two amino-terminal cysteine clusters, $CX_2CX_4CX_3CP$ (residues 40–53 for EhNO1 and residues 41–54 for EhNO2) and $CX_3CX_3CX_3C$ (residues 87–99, EhNO1; 88–100, EhNO2), matched the conserved cysteine-rich patterns proposed to be involved in the formation of [4Fe-4S] clusters (2). Similarly, two regions (residues 137–165 and 264–293 of EhNO1, labeled "FAD-I" and "NAD(P)H", respectively) matched the conserved sequences of an ADP binding fold for the binding of FAD and NAD(P)H. Both EhNO1 and -2 shared features in the NAD(P)H binding domain with the *A. brasilense* GOGAT β-protein (41), which has been proposed to confer

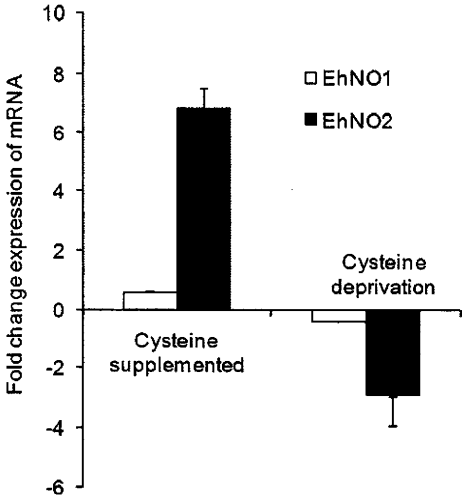

FIGURE 1. **Regulation of gene expression of EhNO isotypes in *E. histolytica* by extracellular L-cysteine concentration.** *E. histolytica* trophozoites were cultured in normal (8 mM), L-cysteine-supplemented (18 mM), or deprived medium. The expression levels of the EhNO transcripts under L-cysteine-supplemented or -deprived conditions were normalized against those of RNA polymerase II and are shown as the -fold change expression of mRNA relative to that of trophozoites from the control (normal) culture. *Error bars* represent the S.E. of three independent experiments.

specificity for NADPH, rather than NADH. The presence of alanine in place of glycine in the last residue of the motif GXGXX(G/A/P) (residues 269–274 of EhNO1 and 270–275 of EhNO2, shown in bold in supplemental Fig. S1) and a conserved arginine in the NAD(P)H binding domain (Arg-293 of EhNO1 and Arg-294 of EhNO2) (42) suggested that the two EhNOs prefer NADPH to NADH as a cofactor. Furthermore, a region in the carboxyl terminus (residues 401–411 of EhNO1 and 402–412 of EhNO2) matched the second FAD binding consensus sequence (TX_8GD).

Phylogenetic Analysis—Phylogenetic reconstruction was performed using neighbor-joining and maximum parsimony programs using 32 GOGAT β subunit or β subunit-like protein sequences from various organisms. The phylogenetic tree constructed using the neighbor-joining method revealed (supplemental Fig. S2) that EhNOs are more closely related to other β subunit-like homologs (supplemental Fig. S2, Group I) than to known GOGAT β subunit proteins (supplemental Fig. S2, Group II). This conclusion was also supported by the phylogenetic reconstruction using the maximum parsimony method (data not shown). Although these data did not clearly indicate the origin of the amebic GOGAT-like proteins, they suggested that EhNOs were most likely obtained by lateral gene transfer from an ancestral organism possessing a Group I-type gene, as reported previously for several other glutamate synthase β subunit-like genes (43).

Regulation of Gene Expression of EhNO Isotypes by L-Cysteine Concentration—To verify the transcriptomic data and confirm that the expression of EhNO1 and -2 was regulated by L-cysteine, the relative steady-state mRNA levels of the EhNO isotypes in *E. histolytica* trophozoites cultivated under L-cysteine-enriched or deprived conditions were measured by quantitative real-time PCR (Fig. 1). Using the RNA polymerase II 15-kDa subunit as an internal control, EhNO2 mRNA increased by

[4] A. Husain, D. Sato, G. Jeelani, M. Suematsu, T. Soga, and T. Nozaki, unpublished information.

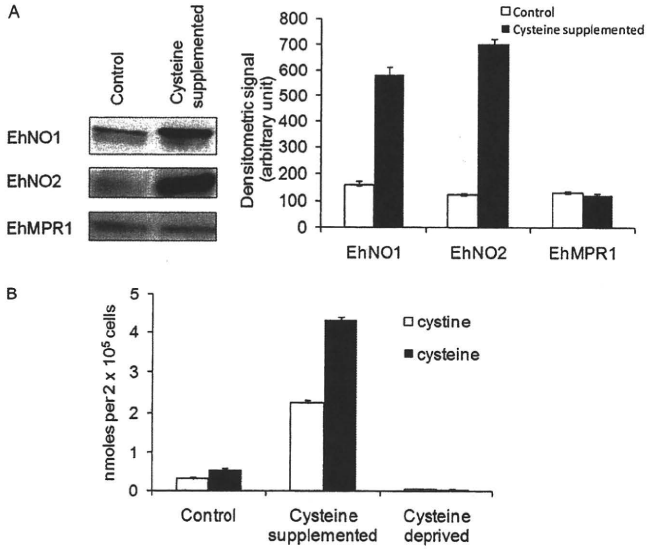

FIGURE 2. **Effects of extracellular L-cysteine concentrations on the amount of EhNO isotypes and intracellular L-cystine/L-cysteine concentrations.** *A*, an immunoblot analysis of EhNO1 and -2 is shown. After trophozoites were cultured under normal or L-cysteine-supplemented conditions for 48 h, ~15 μg of total cell lysate was electrophoresed on a 12% SDS-PAGE gel and subjected to an immunoblot assay with antibodies raised against EhNO1, EhNO2, or EhMPR1 as a control. The densitometric quantification of the reacted bands, shown in the *right graph*, was performed by Scion Image software, and the level of EhNO1, EhNO2, and EhMPR1 proteins was expressed in arbitrary units. *Error bars* represent the S.E. of three independent experiments. *B*, shown is intracellular L-cystine/cysteine concentrations under normal, L-cysteine-supplemented, and deprived conditions. L-Cystine/cysteine concentrations of the trophozoites cultivated for 48 h under the indicated conditions were analyzed by CE-MS. *Error bars* represent the S.E. of three independent experiments.

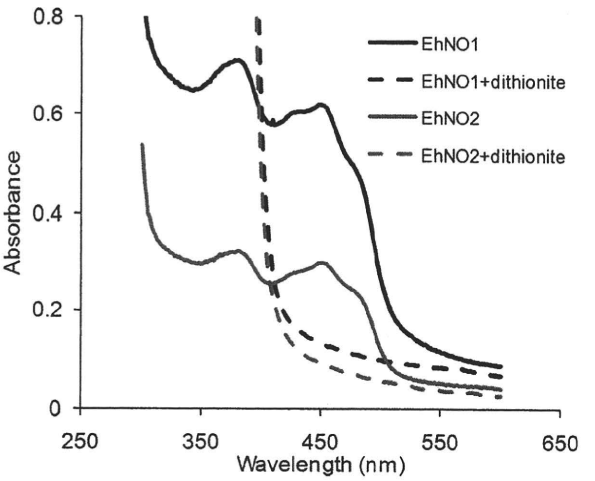

FIGURE 3. **Absorption spectra of rEhNO1 and rEhNO2 proteins.** UV-visible absorption spectra of rEhNO1 (400 μg of protein) and rEhNO2 (200 μg) under non-reducing (*solid lines*) and sodium dithionite-reducing conditions (*broken lines*) are shown. The samples were reduced with a 10-fold molar excess of sodium dithionite.

7-fold when cultured in the presence of 18 mM L-cysteine for 48 h compared with the control condition (8 mM L-cysteine), whereas it was down-regulated by 4-fold when cultured in the absence of L-cysteine. In contrast, the level of EhNO1 remained unchanged in either the presence or absence of L-cysteine.

Expression of EhNO Proteins under L-Cysteine-supplemented and -deprived Conditions—To confirm the changes of *EhNO* transcripts determined by the transcriptomic and real-time PCR analyses, we also examined EhNO expression at the protein level under L-cysteine-supplemented conditions. Immunoblot analysis using anti-rEhNO2 antibody showed that EhNO2 was induced by 6-fold when *E. histolytica* cultures were supplemented with L-cysteine (Fig. 2*A*). Although the RT-PCR results indicated that EhNO1 was not up-regulated under this condition, the protein recognized by anti-EhNO1 antibody was also found to be induced by 3.5-fold. Because anti-EhNO1 and anti-EhNO2 antibodies exhibited cross-reactivity (data not shown), the increased signal of the band recognized by anti-EhNO1 antibody was likely due to cross-reactivity with EhNO2. Alternatively, the level of EhNO1 may have increased by post-transcriptional mechanisms.

Changes in Intracellular L-Cysteine/Cystine Concentrations under L-Cysteine-supplemented and -deprived Conditions—To examine changes in intracellular L-cysteine and L-cystine concentrations caused by L-cysteine supplementation and deprivation, we quantitated their levels using a CE-MS-based approach in trophozoites maintained under normal (8 mM L-cysteine), enriched (18 mM L-cysteine), or deprived conditions. Under normal conditions, the L-cysteine to L-cystine ratio (1.70 ± 0.08) was deviated toward the reduced status. Upon L-cysteine supplementation, the intracellular levels of L-cysteine and L-cystine increased 8.1- and 7.3-fold, respectively, whereas under L-cysteine deprivation, both L-cysteine and L-cystine decreased to undetectable levels (Fig. 2*B*). Under L-cysteine-enriched conditions, the L-cysteine to L-cystine ratio (1.90 ± 0.14) slightly shifted toward the more reduced status (p = 0.031). Because several systems regulate the cellular redox reactions and electrochemical potential of the cell, the observed changes in the L-cysteine/cystine ratio were considered small. Taken together, these data clearly showed that although the extracellular L-cysteine concentration largely affects intracellular L-cysteine/L-cystine levels, its redox equilibrium is not severely affected. Furthermore, it appeared that a significant proportion of the L-cysteine incorporated into the cell was oxidized to L-cystine, which is supported by a previous finding (44). Alternatively, extracellular L-cysteine may be oxidized before uptake and reduced to L-cysteine intracellularly.

Expression and Purification of Recombinant EhNO Isotypes—To determine the biochemical properties of the two EhNO isoenzymes, recombinant proteins were first produced in *E. coli*. SDS-PAGE of the purified rEhNO1 and -2 proteins showed apparently single homogenous bands with molecular weights of 52.2 and 51.9 kDa, respectively, under reducing conditions (supplemental Fig. S3). The observed mobilities of rEhNO1 and -2 were consistent with the predicted sizes of the monomeric EhNO proteins with an extra 3.0-kDa histidine tag added at the amino terminus. The purity of the rEhNOs was estimated to be greater than 95% as judged by densitometric scanning of the stained gel. The rEhNO proteins were stable and retained their full activity for at least 3 months when stored in 10–15% glycerol at -30 or −80 °C.

Prosthetic Groups of rEhNOs—The UV-visible spectra of the purified rEhNOs showed absorbance maxima at 484, 450, 430, 378, and 280 nm (Fig. 3), which are characteristic of iron sulfur

flavoproteins (45). The dithionite-reduced rEhNOs showed, in contrast, a relatively featureless spectrum, with the increased absorbance at shorter wavelengths attributable to dithionite. Denaturation of the rEhNOs by boiling resulted in the release of flavin, indicating that it formed a non-covalent association with the protein. The fluorescence intensity of the free flavin at pH 2.6 was ~4-fold higher than that at pH 7.7 (data not shown). This indicates that FAD, rather than FMN, formed the prosthetic group in rEhNOs. It was calculated that 1.13 ± 0.32 mol of FAD (ϵ of FAD at 450 nm = 11.4×10^3 M^{-1} cm^{-1}) is associated per molecule of rEhNO1, whereas 0.89 ± 0.21 mol of FAD bound per molecule of rEhNO2. The iron analysis using the *O*-phenanthroline method indicated that rEhNO1 contained 7.8 ± 0.62 irons per molecule of rEhNO1, whereas rEhNO2 contained 7.4 ± 0.71 irons per molecule of rEhNO2. These results indicate that two [4Fe-4S] clusters are present per subunit, which is consistent with the $CX_2CX_4CX_3CP$ and $CX_3CX_3CX_3C$ motifs present in EhNO1 and -2. These data together with the stability of the enzymatic activity of rEhNOs also support the premise that rEhNOs retain most, if not all, of the features of the native EhNOs.

Kinetics Properties of rEhNO—The rEhNOs were devoid of glutamate synthase and glutamate dehydrogenase activity in both directions at either pH 7.5 or 9.5. However, both proteins oxidized NADPH and transferred electrons to several alternative electron acceptors, including INT, ferricyanide, and menadione (Table 1). In the presence of NADPH, the reduction rate of INT by rEhNO1 (specific activity 19.42 ± 3.25 μmol min^{-1} mg^{-1}) was >30-fold higher than that by rEhNO2 (0.62 ± 0.10 μmol min^{-1} mg^{-1}), whereas rEhNO2 showed a 2.8-fold higher ferricyanide reducing activity (86.64 ± 8.33 μmol min^{-1} mg^{-1}) than rEhNO1 (31.50 ± 6.21 μmol min^{-1} mg^{-1}). The menadione-reducing activities of rEhNO1 and -2 were comparable (2.48 ± 0.39 and 2.25 ± 0.41 μmol min^{-1} mg^{-1}, respectively). Both rEhNO1 and -2 were highly specific toward NADPH and did not reduce the above-tested electron acceptors with NADH as the electron donor. In the NADPH:flavin oxidoreductase reaction under aerobic conditions, rEhNO1 and -2 produced H_2O_2 at comparable levels (Table 1). Significantly, the two enzymes were also capable of reducing the anti-amebic drug metronidazole and the herbicide paraquat.

In addition to these properties, rEhNO1 and -2 could catalyze the reduction of disulfides, such as L-cystine, which was also dependent on NADPH. The K_m and k_{cat}/K_m values of rEhNO1 and -2 for L-cystine and NADPH were significantly different (Table 2). At substrate-saturating concentrations, the K_m values of rEhNO1 for L-cystine and L-NADPH were 3.3- and 2.3-fold higher, respectively, than those of rEhNO2. The k_{cat}/K_m value of rEhNO2 for L-cystine (measured at saturating concentrations of NADPH) was ~4-fold higher than that of rEhNO1. The addition of *N*-ethylmaleimide, which is commonly used to inhibit sulfydryl-dependent reactions, inhibited the disulfide reducing activities of both rEhNO1 and rEhNO2 (0.5 mM *N*-ethylmaleimide caused 50% inhibition), whereas the presence of up to 5 mM *N*-ethylmaleimide had no effect on the reduction of INT. These results indicate that the two EhNOs contain thiol(s) groups that are involved in disulfide reduction but are not required for their observed oxidoreductase activity (46, 47).

We also found that rEhNO1 and -2 catalyzed the reduction of ferric to ferrous ion. In the presence of NADPH, the reduction rate of Fe(III) by rEhNO1 (k_{cat}/K_m 15.1 ± 3.20 min^{-1} μM^{-1}) was ~116-fold higher than that by rEhNO2 (k_{cat}/K_m 0.12 ± 0.01 min^{-1} μM^{-1}) (Table 2). In addition, both rEhNOs also acted as ferredoxin:$NADP^+$ reductases capable of catalyzing the reduction of $NADP^+$ to NADPH through the utilization of the electrons provided by reduced ferredoxin, although the observed activity of EhNO1 was again higher (7.8-fold) than that of EhNO2. These data suggest that EhNO1 is mainly involved in the reduction of ferric ion and ferrodoxin:$NADP^+$, whereas EhNO2 primarily catalyzes the reduction of L-cystine. The uncatalyzed reaction rate (without enzyme) of each reaction was as follows: 22.5 ± 2.4 pmol/min, INT; 250 ± 32 pmol/min, ferricyanide; 29.2 ± 6.1 pmol/min, menadione; 307 ± 66 pmol/min, paraquat; 22.5 ± 7.8 pmol/min, cystine; 28.9 ± 6.9 pmol/min, ferric ammonium citrate; 6.16 ± 2.7 pmol/min, ferredoxin.

Binary Complexes of EhNO1/2 with Ferredoxins—To examine whether electron transfer between reduced ferredoxin and $NADP^+$ by EhNO1 was dependent on the physical interaction between these two proteins (48), as reported for the spinach leaf redox couple (36), we investigated whether EhNO1 and -2

TABLE 1
Specific activity of purified EhNO1 and EhNO2 with various electron acceptors
Values are expressed as the means ± S.D. of three independent experiments as described under "Experimental Procedures"

Substrate	Specific activity	
	rEhNO1	rEhNO2
	μmol/min/mg	
INT	19.42 ± 3.25	0.62 ± 0.10
Ferricyanide	31.50 ± 6.21	86.64 ± 8.33
Menadione	2.48 ± 0.39	2.25 ± 0.41
Metronidazole	1.75 ± 0.42	1.41 ± 0.46
Paraquat	19.73 ± 4.23	10.60 ± 2.12
Oxygen	8.31 ± 2.12	3.42 ± 0.81

TABLE 2
Kinetic parameters for cystine, ferric, and ferredoxin $NADP^+$ reductase reactions catalyzed by EhNO1 and EhNO2
Values are expressed as the means ± S.D. of three independent experiments.

Substrate	rEhNO1				rEhNO2			
	K_m	V_{max}	k_{cat}	k_{cat}/K_m	K_m	V_{max}	k_{cat}	k_{cat}/K_m
	μM	*μmol/min/mg*	min^{-1}	$min^{-1}\cdot\mu M^{-1}$	*μM*	*μmol/min/mg*	min^{-1}	$min^{-1}\cdot\mu M^{-1}$
Cystine	910 ± 20	0.88 ± 0.06	45.86 ± 7.52	0.05 ± 0.01	276 ± 23	1.15 ± 0.17	59.36 ± 3.81	0.22 ± 0.13
NADPH (cystine)	9.2 ± 2.1	1.70 ± 0.13	88.38 ± 5.83	9.61 ± 1.34	4.2 ± 0.8	1.33 ± 0.43	68.62 ± 5.40	16.33 ± 2.12
Fe(III) citrate	31.3 ± 3.4	9.10 ± 2.51	471.2 ± 17.5	15.1 ± 3.20	98.4 ± 4.5	0.26 ± 0.09	12.18 ± 2.81	0.12 ± 0.01
NADPH (ferric)	70.3 ± 4.9	10.12 ± 3.16	526.6 ± 21.2	7.49 ± 2.12	66.7 ± 8.3	0.72 ± 0.31	37.06 ± 6.28	0.56 ± 0.23
Ferredoxin	0.16 ± 0.05	2.28 ± 0.46	118.8 ± 7.4	742.5 ± 34.1	0.23 ± 0.07	0.43 ± 0.18	21.71 ± 4.51	94.39 ± 8.91

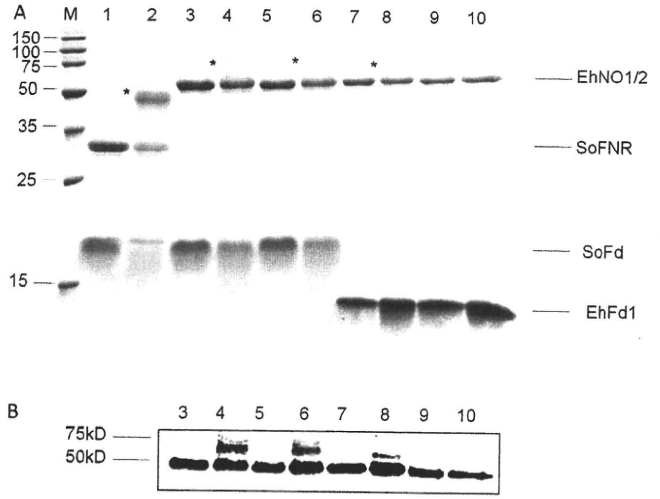

FIGURE 4. ***In vitro* interactions of EhNO with ferredoxin.** *A*, SDS-PAGE analysis of the complex of EhNO and ferredoxin is shown. Protein mixtures were incubated for 30 min with (*even lane numbers*) and without (*odd lane numbers*) 5 mM carbodiimide, electrophoresed on a 15% SDS-PAGE gel under reducing conditions, and then stained with Coomassie Brilliant Blue R250. The examined protein mixtures were as follows: *lanes 1* and *2*, spinach (*S. oleracea*) ferredoxin:NADP$^+$ reductase (*SoFNR*) + spinach ferredoxin (*SoFd*); *lanes 3* and *4*, *EhNO1+SoFd*; *lanes 5* and *6*, *EhNO2+SoFd*; *lanes 7* and *8*, *EhNO1+EhFd1*; *lanes 9* and *10*, *EhNO2+EhFd1*. Protein bands corresponding to the cross-linked proteins are indicated by an *asterisk*. The positions of the purified proteins are indicated on the *right side of the gel*. *B*, shown is an immunoblot analysis of the cross-linked samples using an anti-His antibody.

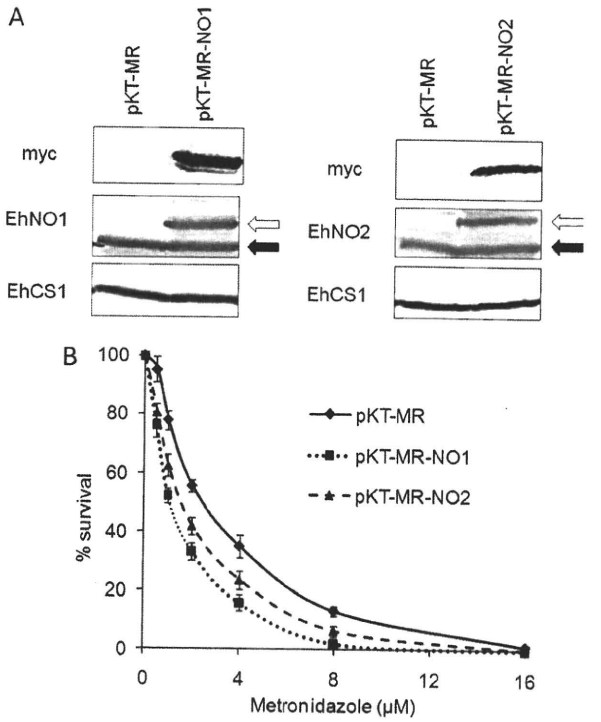

FIGURE 5. **Changes in the sensitivity of *E. histolytica* to metronidazole by overexpression of EhNOs.** *A*, shown is an immunoblot analysis of EhNOs in the transformants expressing Myc-tagged EhNO1 and -2. Approximately 40 μg of total lysate from the pKT-MR (control), EhNO1 (*pKT-MR-NO1*), and EhNO2 (*pKT-MR-NO2*)-overexpressing transformants was electrophoresed on a SDS-PAGE gel under reducing conditions and subjected to immunoblot analysis using anti-EhNO1, anti-EhNO2, anti-Myc, and anti-EhCS1 (*control*) antibodies. *Black* and *white arrows* indicate endogenous and Myc-tagged EhNO1 and -2, respectively. *B*, susceptibility of transformed trophozoites to metronidazole is shown. Trophozoites (10^4 cells/ml) were cultivated in the presence of 0–16 μM metronidazole for 48 h, and the number of viable cells was then counted. The percentages of living cells are shown relative to those of unexposed control cells. *Error bars* represent the S.E. of five independent experiments.

physically interacted with homologous and heterologous (*Spinacia oleracea*) ferredoxin (SoFd) using a carbodiimide-promoted cross-linking (50). We first cloned and purified a representative [3Fe4S] ferredoxin found in the *E. histolytica* genome data base (EhFd1; TIGR ID 128.m00136). For the assay, rEhNO1 and -2 were mixed with either purified EhFd1 or SoFd, cross-linked, and then analyzed by SDS-PAGE (Fig. 4*A*). It was observed that both rEhNO1 and -2 formed a complex with spinach ferredoxin, as shown by the appearance of a large 60-kDa band in the gel and more easily observed in the Western blot analysis using an anti-histidine antibody (Fig. 4*B*, *lanes 4* and *6*). However, only EhNO1 formed a complex with *E. histolytica* ferredoxin (EhFd1) (Fig. 4, *A* and *B*, *lanes 8* and *10*).

Cellular Distribution of EhNO—We also examined the cellular distribution of EhNO1 and -2 in trophozoites. The immunofluorescence imaging using antiserum raised against the corresponding recombinant protein revealed that the two isotypes were distributed throughout the cytosol (data not shown). We also verified the localization of EhNOs by immunoblotting using lysates produced by a Dounce glass homogenizer followed by sonication and centrifugation at 100,000 × *g* at 4 °C for 1 h. Both EhNO1 and -2 fractionated into the soluble fraction (data not shown).

Increased Metronidazole Sensitivity by EhNO Overexpression—To confirm that EhNO is the target of metronidazole in *E. histolytica*, stable transformants that overexpressed Myc-tagged EhNO1 or 2 were generated. Both the transformants expressing Myc-tagged EhNO1 or EhNO2 expressed ~2-fold higher levels of the corresponding enzymes than the control (Fig. 5*A*) and were more sensitive to metronidazole. The 50% growth inhibitory concentrations (IC_{50}) of metronidazole for the Myc-EhNO1- and Myc-EhNO2-overexpressing transformants were 1.03 ± 0.05 and 1.42 ± 0.12 μM, respectively (Fig. 5*B*), whereas the control showed an IC_{50} of 2.24 ± 0.33 μM.

DISCUSSION

In the present study we demonstrated novel enzymatic reactions catalyzed by a new class of FAD- and 2[4Fe-4S]-containing NADPH-dependent oxidoreductases from *E. histolytica*, which had been initially discovered by virtue of tightly regulated gene expression in correlation with L-cysteine concentrations. Although the two EhNOs characterized in this study had been annotated before this study based on their high degree of homology with GOGAT β subunit and β subunit-like genes from a variety of organisms, their biochemical function was unknown. The fact that the two EhNOs shared significant similarity with homologs from archaeal organisms raised the question of whether they represented a prototype GOGAT protein, similar to the β subunit protein from *Pyrococcus*, which was reported to possess NADPH-dependent GOGAT activity and be capable of both glutamine and ammonia-dependent synthesis in the absence of the α subunit (7). However, we were unable to observe glutamate synthase activity of the EhNOs under similar conditions used for the *Pyrococcus* glutamate synthase. Fur-

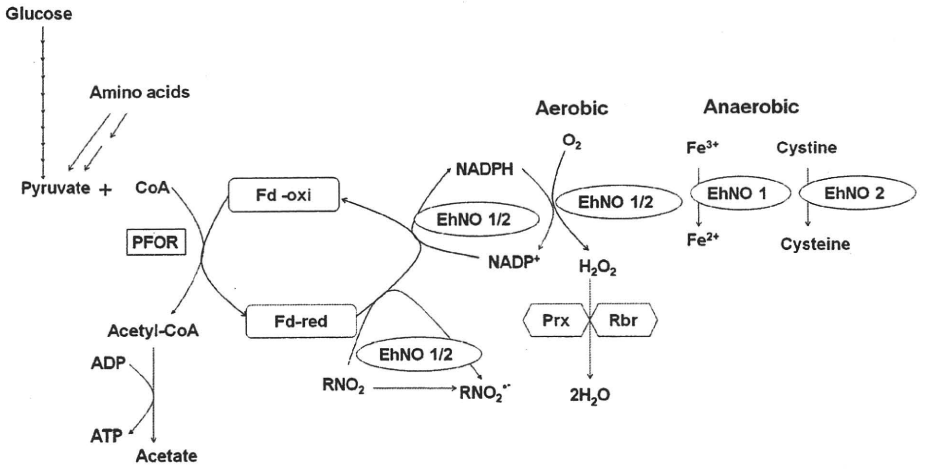

FIGURE 6. **Proposed *in vivo* reactions catalyzed by EhNO1 and -2.** *PFOR*, pyruvate:ferredoxin oxidoreductase; *Fd-red* and *Fd-oxi*, reduced and oxidized form of ferredoxin; *Prx*, peroxiredoxin; *Rbr*, rubrerythrin; *RNO_2/$RNO_2^{\bullet}$*, metronidazole/reduced metronidazole.

thermore, the expression of the GOGAT β subunit failed to restore glutamate auxotrophy in an *E. coli* GOGAT α subunit-deficient strain (5, 51). In addition, it was somewhat puzzling how the *Pyrococcus* GOGAT β subunit functioned in substrate binding and catalysis without the α subunit, which has been shown to be responsible for substrate recognition (52). Thus, it was thought that the EhNO β subunit-like proteins may be involved in reactions other than glutamate synthesis.

The physiological roles of EhNO1 and EhNO2 have not been unequivocally demonstrated because our attempt to repress EhNO expression by gene silencing (53) failed (data not shown), and gene knock-out has not been accomplished in *E. histolytica*. Nevertheless, our present enzymological characterization revealed the physiological significance of the presence of the two isotypes of EhNOs. EhNO2 appears to play an important role in the reduction of cystine to L-cysteine. Because L-cysteine is partially present in the oxidized form inside cells (CE-MS analysis, Fig. 2*B*), L-cystine reduction is necessary before the utilization of L-cysteine, which has been implicated in the attachment to matrix, elongation, motility, growth, and anti-oxidative defense (35, 54, 55). Transcriptomic analysis demonstrated that the transcription of EhNO2, but not EhNO1, is tightly regulated by extracellular L-cysteine concentrations. Furthermore, the measured kinetic parameters indicate that EhNO2 possesses 4-fold higher L-cystine reduction efficiency than EhNO1.

The acquisition of iron and subsequent assimilation into cellular proteins are ubiquitously essential for life. However, at physiological pH under aerobic conditions, iron is present as Fe^{3+} hydroxides and oxyhydroxides or in a complex with ferric-specific chelators, *e.g.* siderophores (56). Subsequent reduction of complexed Fe^{3+} is accomplished by ferric reductases using NAD(P)H as the electron donor (57), with the resulting Fe^{2+} being subsequently released and incorporated into iron-containing proteins (58). We showed that rEhNO1 catalyzes the reduction of ferric ion >100-fold more efficiently than rEhNO2 (Table 2), suggesting that EhNO1 is mainly involved in ferric reduction. We also confirmed that EhNO1 functions as a ferredoxin:$NADP^+$ reductase, similar to the recently reported ferric reductase from *Pseudomonas putida* (59), by catalyzing reversible electron transfer between one molecule of $NADP^+$/NADPH and two molecules of ferredoxin. *In vitro* cross-linking of the two EhNOs with ferredoxin indicate that only EhNO1 forms a stable complex with *E. histolytica* ferredoxin (EhFd1), whereas both EhNO1 and EhNO2 physically interact with spinach ferredoxin (Fig. 4*B*), indicating that the specificity toward ferredoxin differs between these two proteins. The *E. histolytica* genome encodes four types of ferredoxins which are highly divergent at the primary sequence level and also in the Fe-S clusters. We, therefore, hypothesize that EhNO2 interacts with a ferredoxin(s) other than EhFd1 in *E. histolytica*, a speculation that is supported by the observed differential binding of photosynthetic and non-photosynthetic maize ferredoxins to root *Zea mays* ferredoxin:$NADP^+$ reductase (60).

E. histolytica is anaerobic/microaerophilic and possesses highly degenerated mitochondria that are incapable of oxidative phosphorylation and ATP generation. A crucial step in energy production via glycolysis and fermentation in *E. histolytica* involves the decarboxylation of pyruvate to acetyl CoA that is catalyzed by pyruvate:ferredoxin oxidoreductase (61). Concomitant with the decarboxylation of pyruvate, an electron is transferred to oxidized ferredoxin. Generally, reduced ferredoxin subsequently donates an electron to NAD(P) by the action of ferredoxin:NADP reductase, which serves to regenerate the intracellular pools of NAD(P)H and oxidized ferredoxin. However, as the *Entamoeba* genome does not contain an ferredoxin:NADP reductase homolog, it was unclear how NAD(P)H was regenerated. Our enzymological study indicates that EhNOs, and EhNO1 in particular, function as ferredoxin:NADP reductases and are involved in the regeneration of NADPH and oxidized ferredoxin required for continuous energy production.

As stated above, *E. histolytica* possesses highly divergent mitochondria (62) and lacks a functional tricarboxylic acid cycle, cytochromes, and a conventional respiratory electron transport chain terminating in the reduction of oxygen to water. However, amebae can still tolerate up to 5% of oxygen in the gas phase (63, 64) and consume oxygen (65). As shown here, EhNOs are flavoproteins containing 1 mol of FAD as a prosthetic group per mol of enzyme. During the NADPH:flavin oxidoreductase reaction, NADPH binds to EhNOs, and two electrons are transferred to FAD to yield $FADH_2$, which is immediately dissociated from the enzyme (66). Under aerobic conditions, $FADH_2$ is rapidly oxidized by molecular oxygen to yield H_2O_2 and FAD (67). As *E. histolytica* amebae do not produce detectable amounts of H_2O_2 (27), it is possible that H_2O_2 is further converted to water by peroxiredoxin (68) and rubrerythrin (69) to overcome oxidative stress. Under anaero-

bic conditions, EhNO1 catalyzes ferric ion reduction, whereas EhNO2 catalyzes cystine reduction. Based on the demonstrated reactions catalyzed by the two EhNOs, we have proposed functional roles for these two proteins in *E. histolytica* that are summarized in Fig. 6.

Metronidazole is a prodrug currently used to treat a number of microbial infections, and its activation requires intracellular reduction to produce cytotoxic short-lived radicals and other reactive species (70). *Entamoeba* electron transport proteins, which have been reported to provide the source of electrons for the reductive activation of metronidazole, include ferredoxin (71), thioredoxin reductase (72), and nitroreductase (49). We demonstrated that both EhNO1 and -2 catalyze metronidazole reduction *in vitro* (Table 1), and their overexpression confers increased sensitivity to this drug (Fig. 5*B*). This finding suggests that in addition to ferredoxin (71), pyruvate:ferredoxin oxidoreductase (71), thioredoxin (72), and nitroreductase (49), EhNO1 and -2 are also involved in metronidazole activation in *E. histolytica*.

In conclusion, we have demonstrated for the first time that two novel NADPH-dependent GOGAT small subunit-like proteins of *E. histolytica* function, at least *in vitro*, as cystine/ferric/ferredoxin:$NADP^+$ reductase. We propose that they play a role in maintaining intracellular redox potential and may be responsible for metronidazole activation in this parasite. The physiological substrates and biological roles of the majority of oxidoreductases discovered by genome mining remain largely unknown. Vigorous attempts to discover the substrates and functions of individual oxidoreductases should unveil novel cellular metabolic processes in pathogens and cancer cells that may lead to the development of new chemotherapeutics.

Acknowledgments—We thank Kumiko Nakada-Tsukui, Fumika Michi, Takashi Makiuchi, and all other members of our laboratory for technical assistance and valuable discussions.

REFERENCES

1. Ratti, S., Curti, B., Zanetti, G., and Galli, E. (1985) *J. Bacteriol.* **163,** 724–729
2. Rosenbaum, K., Jahnke, K., Curti, B., Hagen, W. R., Schnackerz, K. D., and Vanoni, M. A. (1998) *Biochemistry* **37,** 17598–17609
3. Tóth, A., Takács, M., Groma, G., Rákhely, G., and Kovács, K. L. (2008) *FEMS Microbiol. Lett.* **282,** 8–14
4. Vanoni, M. A., and Curti, B. (1999) *Cell Mol. Life Sci.* **55,** 617–638
5. Stutz, H. E., and Reid, S. J. (2004) *Biochim. Biophys. Acta* **1676,** 71–82
6. Saum, S. H., Sydow, J. F., Palm, P., Pfeiffer, F., Oesterhelt, D., and Müller, V. (2006) *J. Bacteriol.* **188,** 6808–6815
7. Jongsareejit, B., Rahman, R. N., Fujiwara, S., and Imanaka, T. (1997) *Mol. Gen. Genet.* **254,** 635–642
8. World Health Organization (1997) *WHO/PAHO/UNESCO Report: A consultation with experts on amebiasis. Mexico City, Mexico 28–29 January, 1997. Epidemiol. Bull* **18,** 13–14
9. Upcroft, P., and Upcroft, J. A. (2001) *Clin. Microbiol. Rev.* **14,** 150–164
10. Hoffman, J. S., and Cave, D. R. (2001) *Curr. Opin. Gastroenterol.* **17,** 30–34
11. World Health Organization (2007 March) *WHO Model List of Essential Medicines,* 15th Ed.
12. Müller, M. (1983) *Surgery* **93,** 165–171
13. Moreno, S. N., and Docampo, R. (1985) *Environ. Health Perspect.* **64,** 199–208
14. West, S. B., Wislocki, P. G., Fiorentini, K. M., Alvaro, R., Wolf, F. J., and Lu,, A. Y. (1982) *Chem. Biol. Interact.* **41,** 265–279
15. Ludlum, D. B., Colinas, R. J., Kirk, M. C., and Mehta, J. R. (1988) *Carcinogenesis* **9,** 593–596
16. Diamond, L. S., Harlow, D. R., and Cunnick, C. C. (1978) *Trans. R. Soc. Trop. Med. Hyg.* **72,** 431–432
17. Clark, C. G., and Diamond, L. S. (2002) *Clin. Microbiol. Rev.* **15,** 329–341
18. Thompson, J. D., Higgins, D. G., and Gibson, T. J. (1994) *Nucleic Acids Res.* **22,** 4673–4680
19. Leão-Helder, A. N., Krikken, A. M., Gellissen, G., van der Klei, I. J., Veenhuis, M., and Kiel, J. A. (2004) *FEBS Lett.* **577,** 491–495
20. Kumar, S., Tamura, K., Jakobsen, I. B., and Nei, M. (2001) *Bioinformatics* **17,** 1244–1245
21. Sambrook, J., and Russell, D. W. (2001) *Molecular Cloning: A Laboratory Manual,* 3rd Ed., Cold Spring Harbor Laboratory Press, Cold Spring Harbor, NY
22. Nozaki, T., Asai, T., Kobayashi, S., Ikegami, F., Noji, M., Saito, K., and Takeuchi, T.. (1998) *Mol. Biochem. Parasitol.* **97,** 33–44
23. Bradford, M. M. (1976) *Anal. Biochem.* **72,** 248–254
24. Faeder, E. J., and Siegel, L. M. (1973) *Anal. Biochem.* **53,** 332–336
25. Olson, J. W., Agar, J. N., Johnson, M. K., and Maier, R. J. (2000) *Biochemistry* **39,** 16213–16219
26. Chen, J. S., and Blanchard, D. K. (1979) *Anal. Biochem.* **93,** 216–222
27. Lo, H., and Reeves, R. E. (1980) *Mol. Biochem. Parasitol.* **2,** 23–30
28. Ichikawa, Y., Hiwatashi, A., Yamano, T., Kim, H. J., and Maruya, N. (1980) in *Flavins and Flavoproteins* (Yagi, K., and Yamano, T., eds) pp. 677–691, University Park Press, Baltimore, MD
29. Thurman, R. G., Ley, H. G., and Scholz, R. (1972) *Eur. J. Biochem.* **25,** 420–430
30. Soga, T., and Heiger, D. N. (2000) *Anal. Chem.* **72,** 1236–1241
31. Soga, T., Ohashi, Y., Ueno, Y., Naraoka, H., Tomita, M., and Nishioka, T. (2003) *J. Proteome Res.* **2,** 488–494
32. Soga, T., Baran, R., Suematsu, M., Ueno, Y., Ikeda, S., Sakurakawa, T., Kakazu, Y., Ishikawa, T., Robert, M., Nishioka, T., and Tomita, M. (2006) *J. Biol. Chem.* **281,** 16768–16776
33. Ohashi, Y., Hirayama, A., Ishikawa, T., Nakamura, S., Shimizu, K., Ueno, Y., Tomita, M., and Soga, T. (2008) *Mol. Biosyst.* **4,** 135–147
34. Nakada-Tsukui, K., Okada, H., Mitra, B. N., and Nozaki, T. (2009) *Cell. Microbiol.* **11,** 1471–1491
35. Nozaki, T., Asai, T., Sanchez, L. B., Kobayashi, S., Nakazawa, M., and Takeuchi, T. (1999) *J. Biol. Chem.* **274,** 32445–32452
36. Zanetti, G., Morelli, D., Ronchi, S., Negri, A., Aliverti, A., and Curti, B. (1988) *Biochemistry* **27,** 3753–3759
37. Tokoro, M., Asai, T., Kobayashi, S., Takeuchi, T., and Nozaki, T. (2003) *J. Biol. Chem.* **278,** 42717–42727
38. Nakada-Tsukui, K., Saito-Nakano, Y., Ali, V., and Nozaki, T. (2005) *Mol. Biol. Cell* **16,** 5294–5303
39. Srivastava, M., Ahmad, N., Gupta, S., and Mukhtar, H. (2001) *J. Biol. Chem.* **276,** 15481–15488
40. Loftus, B., Anderson, I., Davies, R., Alsmark, U. C., Samuelson, J., Amedeo, P., Roncaglia, P., Berriman, M., Hirt, R. P., Mann, B. J., Nozaki, T., Suh, B., Pop., M., Duchene, M., Ackers, J., Tannich, E., Leippe, M., Hofer, M., Bruchhaus, I., Willhoeft, U., Bhattacharya, A., Chillingworth, T., Churcher, C., Hance, Z., Harris, B., Harris, D., Jagels, K., Moule, S., Mungall, K., Ormond, D., Squares, R., Whitehead, S., Quail, M. A., Rabbinowitsch, E., Norbertczak, H., Price, C., Wang, Z., Guillén, N., Gilchrist, C., Stroup, S. E., Bhattacharya, S., Lohia, A., Foster, P. G., Sicheritz-Ponten, T., Weber, C., Singh, U., Mukherjee, C., El-Sayed, N. M., Petri, W. A., Jr, Clark, C. G., Embley, T. M., Barrell, B., Fraser, C. M., and Hall, N. (2005) *Nature* **433,** 865–868
41. Morandi, P., Valzasina, B., Colombo, C., Curti, B., and Vanoni, M. A. (2000) *Biochemistry* **39,** 727–735
42. Pelanda, R., Vanoni, M. A., Perego, M., Piubelli, L., Galizzi, A., Curti, B., and Zanetti, G. (1993) *J. Biol. Chem.* **268,** 3099–3106
43. Andersson, J. O., and Roger, A. J. (2002) *Eukaryot. Cell* **1,** 304–310
44. Gillin, F. D., and Diamond, L. S. (1981) *Exp. Parasitol.* **51,** 382–391
45. Latimer, M. T., Painter, M. H., and Ferry, J. G. (1996) *J. Biol. Chem.* **271,** 24023–24028
46. Fontecave, M., Eliasson, R., and Reichard, P. (1987) *J. Biol. Chem.* **262,** 12325–12331

47. Jablonski, E., and DeLuca, M. (1978) *Biochemistry* **17,** 672–678
48. Foust, G. P., Mayhew, S. G., and Massey, V. (1969) *J. Biol. Chem.* **244,** 964–970
49. Pal, D., Banerjee, S., Cui, J., Schwartz, A., Ghosh, S. K., and Samuelson, J. (2009) *Antimicrob. Agents Chemother.* **53,** 458–464
50. Zanetti, G., Aliverti, A., and Curti, B. (1984) *J. Biol. Chem.* **259,** 6153–6157
51. Deane, S. M., and Rawlings, D. E. (1996) *Gene* **177,** 261–263
52. Vanoni, M. A., Fischer, F., Ravasio, S., Verzotti, E., Edmondson, D. E., Hagen, W. R., Zanetti, G., and Curti, B. (1998) *Biochemistry* **37,** 1828–1838
53. Bracha, R., Nuchamowitz, Y., Anbar, M., and Mirelman, D. (2006) *PLoS Pathog.* **2,** e48
54. Gillin, F. D., and Diamond, L. S. (1981) *Exp. Parasitol.* **52,** 9–17
55. Gillin, F. D., and Diamond, L. S. (1980) *J. Protozool.* **27,** 474–478
56. Barchini, E., and Cowart, R. E. (1996) *Arch. Microbiol.* **166,** 51–57
57. Lesuisse, E., Crichton, R. R., and Labbe, P. (1990) *Biochim. Biophys. Acta* **1038,** 253–259
58. Guerinot, M. L. (1994) *Annu. Rev. Microbiol.* **48,** 743–772
59. Yeom, J., Jeon, C. O., Madsen, E. L., and Park, W. (2009) *J. Bacteriol.* **191,** 1472–1479
60. Onda, Y., Matsumura, T., Kimata-Ariga, Y., Sakakibara, H., Sugiyama, T., and Hase, T. (2000) *Plant Physiol.* **123,** 1037–1045
61. Kerscher, L., and Oesterhelt, D. (1982) *Trends Biol. Sci.* **7,** 371–374
62. Tovar, J., Fischer, A., and Clark, C. G. (1999) *Mol. Microbiol.* **32,** 1013–1021
63. Band, R. N., and Cirrito, H. (1979) *J. Protozool.* **26,** 282–286
64. Reeves, R. E. (1984) *Adv. Parasitol.* **23,** 105–142
65. Weinbach, E. C., and Diamond, L. S. (1974) *Exp. Parasitol.* **35,** 232–243
66. Inouye, S. (1994) *FEBS Lett.* **347,** 163–168
67. Gibson, Q. H., and Hastings, J. W. (1962) *Biochem. J.* **83,** 368–377
68. Bruchhaus, I., Richter, S., and Tannich, E. (1997) *Biochem. J.* **326,** 785–789
69. Maralikova, B., Ali, V., Nakada-Tsukui, K., Nozaki, T., van der Giezen, M., Henze, K., and Tovar, J. (2010) *Cell Microbiol.* **12,** 331–342
70. Goldman, P., Koch, R. L., Yeung, T. C., Chrystal, E. J., Beaulieu, B. B., Jr., McLafferty, M. A., and Sudlow, G. (1986) *Biochem. Pharmacol.* **35,** 43–51
71. Müller, M. (1986) *Biochem. Pharmacol.* **35,** 37–41
72. Leitsch, D., Kolarich, D., Wilson, I. B. H., Altmann, F., and Duchene, M. (2007) *PLoS Biol.* **5,** e211

Experimental Parasitology 125 (2010) 279–285

Contents lists available at ScienceDirect

Experimental Parasitology

journal homepage: www.elsevier.com/locate/yexpr

Entamoeba histolytica: Molecular cloning and characterization of a novel neutral sphingomyelinase

Claudia Leticia Mendoza-Macías [a], Minerva Paola Barrios-Ceballos [a], Fernando Anaya-Velázquez [a], Kumiko Nakada-Tsukui [b], Tomoyoshi Nozaki [b], Felipe Padilla-Vaca [a,*]

[a] Departamento de Biología, División de Ciencias Naturales y Exactas, Universidad de Guanajuato, Guanajuato 36050, Mexico
[b] Department of Parasitology, National Institute of Infectious Diseases, Shinjuku-ku, Tokyo 162-8640, Japan

ARTICLE INFO

Article history:
Received 4 November 2009
Received in revised form 28 January 2010
Accepted 1 February 2010
Available online 6 February 2010

Keywords:
Entamoeba histolytica
Sphingomyelinase
Ceramide
Scyphostatin

ABSTRACT

A novel neutral sphingomyelinase (nSMase) was characterized in *Entamoeba histolytica* trophozoites. SMase, a sphingomyelin-specific form of phospholipase C, catalyzes the hydrolysis of sphingomyelin to ceramide and phosphorylcholine. Three amebic putative nSMase genes were found to be actively transcribed. Mg^{2+}-independent nSMase activity in the soluble fraction of the trophozoites was stimulated by Mn^{2+} and partially inhibited by Zn^{2+}. nSMase activity of the recombinant protein EhnSM1, increased 4.5-fold in the presence of 0.5 mM Mn^{2+}, and abolished by 5 mM Zn^{2+}. A dose-dependent inhibition of rEhnSM1 was observed with scyphostatin, a specific inhibitor of nSMases. The EhnSM1 and EhnSM3 were detected in the soluble fraction of the amebic lysate as 35–37 kDa proteins by western blot analysis. Immunofluorescence assay showed that the overexpressed HA-tagged EhnSM1 and EhnSM3 were localized to the cytosol. The biological role of these novel *E. histolytica* nSMases described in this work remains to be determined.

1. Introduction

Sphingomyelinases (SMases), sphingomyelin-specific forms of phospholipases C, are phosphodiesterases that catalyze the hydrolysis of sphingomyelin (SM) in biological membranes to ceramide and phosphorylcholine. SMases can be classified by their optimum pH in acidic, neutral and alkaline SMases (Steinbrecher et al., 2004; Schenck et al., 2007). In mammals, neutral SMases (nSMases) are located in the plasma membrane and cytosol; the acidic SMases (aSMases) are present in the lumen of endosomes, phagosomes and lysosomes, and at the outer leaflet of the plasma membrane; and alkaline SMases are localized in intestinal mucosa and bile (Krönke, 1999; Grassme et al., 2001). nSMases and aSMases are involved in signal transduction in mammalian cells (Marchesini and Hannun, 2004), whereas alkaline SMases are responsible for digestion of dietary sphingomyelin in the intestine and may protect it from inflammation and tumorigenesis (Wu et al., 2006). Ceramide generated by the activity of nSMase and aSMase has been shown by many studies to play a pivotal role in sphingolipid metabolism, the immediate stress response, and in apoptotic stimuli in almost any mammalian cell (Schenck et al., 2007). Ceramide reorganizes cell membranes and forms larger ceramide-enriched membrane platforms that are required for diverse signal transduction (Schenck et al., 2007; Zhang et al., 2008).

Although mammalian SMases are the most studied, several types of enzymes with SMase C activity have been identified in other eukaryotes as well as in prokaryotes. SC1, the *Saccharomyces cerevisiae* homologue of mammalian nSMases, acts on complex sphingolipids. Yeasts do not have sphingomyelin but instead have inositol phosphosphingolipids, which may function as orthologs of mammalian sphingomyelin to produce the bioactive ceramide (Matmati and Hannun, 2008). A number of pathogenic bacteria, such as *Staphylococcus aureus* (Projan et al., 1989), *Bacillus cereus* (Yamada et al., 1988), *Leptospira interrogans* (Segers et al., 1990) and *Listeria ivanovii* (González-Zorn et al., 1999), secrete nSMases C that act as membrane damaging virulence factors. Bacterial and eukaryotic SMases C share a similar catalytic mechanism and overall structure (Goñi and Alonso, 2002; Sueyoshi et al., 2002; Openshaw et al., 2005).

Sphingolipid metabolism is important in various cellular events in parasites, such as *Giardia lamblia* and *Plasmodium falciparum*. *G. lamblia* synthesizes SMase encoded by *gsmase B* and *gsmase 3b* during encystation to generate additional ceramide, which is not syn-

Abbreviations: SM, sphingomyelin; PS, phosphatidylserine; SMase, sphingomyelinase; nSMase, neutral sphingomyelinase; aSMase, acidic sphingomyelinase; HA, hemagglutinin; rEhnSM1, recombinant protein EhnSM1; PBS, phosphate-buffered saline; RT-PCR, reverse transcriptase polymerase chain reaction; ROS, reactive oxygen species; RNS, reactive nitrogen species; IFA, immunofluorescence assay.

* Corresponding author. Address: Departamento de Biología, División de Ciencias Naturales y Exactas, Universidad de Guanajuato, Noria Alta s/n. Guanajuato, Gto. 36050, Mexico. Fax: +52 473 7320006x8153.
E-mail address: padillaf@quijote.ugto.mx (F. Padilla-Vaca).

0014-4894/$ - see front matter © 2010 Elsevier Inc. All rights reserved.
doi:10.1016/j.exppara.2010.02.001

thesized de novo (Hernandez et al., 2008). *P. falciparum* has a membrane-associated nSMase activity, which is dependent on Mg^{2+} and anionic phospholipids, and involved in the sphingomyelin catabolism (Hanada et al., 2000). It has been suggested that ceramide might modulate the progression of the cell cycle of this parasite (Hanada et al., 2002) as it has been demonstrated for mammalian and yeast cells (Marchesini and Hannun, 2004; Matmati and Hannun, 2008).

Entamoeba histolytica is a human intestinal protozoan parasite and the causative agent of amebiasis, responsible for up to 100,000 deaths each year (WHO, 1997). Only 10% of infections result in invasive disease, but the reasons behind this phenomenon remain largely unknown (Haque et al., 2002). Although little is known about sphingolipid metabolism in this parasite, pathogenic *Entamoeba* synthesizes several sphingolipids such as sphingomyelin, inositol phosphate ceramide and ethanolamide-phosphate ceramide (McLaughlin and Meerovitch, 1975; Alley et al., 1980). As in mammalian cells, amebic sphingomyelin-rich structures in membrane (rafts) are associated with adhesion to target cells and pinocitosis (Laughlin et al., 2004; Mittal et al., 2008). In *Entamoeba invadens*, a related parasite, intermediate metabolites of sphingomyelin synthesis are important for cell proliferation (Cerbón et al., 2009). However, it remains unknown whether the pathogenic parasite *E. histolytica* has SMase activity, an enzyme that plays a key role in sphingolipid metabolism and involved in several important cell functions. In the present work, a novel nSMase activity was detected and characterized in the parasite. We also describe the molecular cloning, characterization of recombinant nSMase expressed in *Escherichia coli*, and cellular localization in trophozoites of *E. histolytica*.

2. Materials and methods

2.1. Ameba culture and cell fractionation

Trophozoites of *E. histolytica* HM-1:IMSS were cultured under axenic conditions in Diamond's TYI-S-33 medium (Diamond et al., 1978). The parasites were harvested at the exponential phase of growth, washed twice with a solution of phosphate-buffered saline (PBS), pH 7.0. Trophozoites were re-suspended (5×10^6 cell/ml) in lysis buffer (100 mM Tris–HCl pH 7.4 plus 0.05 mM E64) and disrupted with hand homogenizer, followed by three freeze–thawing cycles. The homogenate was centrifuged at 40,000×*g* for 1 h at 4 °C. The pellet was solubilized with lysis buffer containing 1% Triton X-100. The supernatant and solubilized pellet were used for further experiments.

2.2. Assay of sphingomyelinase activity

The activity of nSMase was routinely determined using an Amplex® Red Sphingomyelinase Assay Kit (Molecular Probes) as directed by the manufacturer. Briefly, 25 µl of 100 mM Tris–HCl buffer (pH 7.5) containing sphingomyelin (0.5 mM), 2% Triton X-100, 100 mM Amplex red reagent, 2 U mL^{-1} horseradish peroxidase, 0.2 U mL^{-1} choline oxidase and 8 U mL^{-1} alkaline phosphatase, were mixed with 25 µl of 100 mM Tris–HCl (pH 7.5) containing enzymatic source (total lysate, cell fractionations or recombinant protein). After incubation for 20 min at 37 °C, the fluorescence at 582 nm was measured, with excitation at 556 nm, using a Perkin-Elmer LS-5B luminescence spectrometer. In all the assays, background from the enzyme-free controls, in which vehicle buffers instead of the enzyme sources were added, were routinely subtracted from the activities of samples containing enzyme sources.

2.3. Reverse transcriptase polymerase chain reaction

Total RNA was isolated from amebic trophozoites with the Aurum Total RNA Mini Kit (BIO-RAD) including DNAase treatment as directed by the manufacturer. For the synthesis of first strand cDNA, 3 µg of total RNA (DNA-free) isolated from amebic trophozoites were reverse transcribed using oligo(dT) and reverse transcriptase from ThermoScript RT-system (Invitrogen). Reverse transcription was carried out for 90 min at 42 °C with a final denaturation at 94 °C for 2 min. Fivefold dilutions of cDNA were used as template for 35 cycles of linear PCR amplification with specific primers for SMases sequences reported at the genome database from *E. histolytica*. PCR products were fractionated on 1% agarose gels, stained with ethidium bromide, and photographed with a KODAK Image Station 2000R.

2.4. Plasmid constructs and recombinant SMases production

DNA encoding amebic SMases was generated by PCR from *E. histolytica* HM1:IMSS cDNA. EhnSM1 coding region (EHI_007460) was amplified using primers 5′-CCG*GAATTC*CGAACAATCCCCTTCAT-3′ and 5′-CCC*AAGCTT*TTACAATAATTCTAGTGT-3′; for EhnSM3 (EHI_125790), primers 5′-CGC*GGATCC*GCAGAAGAAGCCATT-3′ and 5′-CC*CAAGCTT*AAGATAAACGTCACATG-3′ were used. Sense and antisense primers contain *BamH*I and *Hind*III restriction sites (italicized), respectively for subsequent cloning. PCR products were cloned into pGEM-T (Novagen) and subcloned into pRSET (Invitrogen). The resulting plasmids pRSET-nSM1 and pRSET-nSM3 encoding an EhnSMase linked to a histidine tag were sequenced and used to transform *E. coli* BL21 AI cells (Invitrogen). For overexpression of recombinant SMases, BL21 AI cultures were grown to a density of ~0.4–0.6 OD 600 at 37 °C, induced with 0.2% L-arabinose (final concentration), and cultured for 3 h at 37 °C. To maximize the yield of recombinant soluble proteins, *E. coli* cells were cultured for 8 h at 20 °C.

2.5. SMase antibodies production and western blotting

Recombinant SMases, rEhnSM1 and rEhnSM3, were purified under denaturing conditions by Ni-NTA Agarose (Qiagen) as directed by the manufacturer for production of polyclonal antibodies. Purified enzymes were subjected to 10% SDS–PAGE and stained with 0.1% Coomassie blue in water. The SMase band in each case was excised, homogenized, and used to immunize a rabbit three times, with a month interval following a modified method (Larsson and Sjoquist, 1988). Immune sera were obtained after lethal punction of rabbits. Western blotting was performed using polyclonal rabbit anti-SMase antibodies as primary antibodies and horseradish peroxidase-conjugated goat anti-rabbit IgG (Amersham Pharmacia Biotech) as a secondary antibody, and visualized using the ECL kit (Amersham Pharmacia Biotech). Protein concentration was determined by the DS Protein Assay (Bio-Rad).

2.6. Purification of a recombinant nSMase and functional characterization

Soluble recombinant protein EhnSM1 was purified under native conditions for detection of SMase activity. Briefly, harvested *E. coli* BL21 AI cells were suspended with 50 mM NaH_2PO_4, 300 mM NaCl, 10 mM imidazole (pH 8) at 2 ml per gram of wet weight. Egg white lysozyme was added to the cell suspension at a final concentration of 10 mg/ml, and the mixture was incubated 30 min following three freeze–thawing cycles. The cell lysate was centrifuged at 10,000×*g* for 20 min, and the rEhnSM1 protein was purified from the supernatant fraction using Ni-NTA Agarose (Qiagen) as directed by manufacturer. The purified protein was applied to a Hi Trap

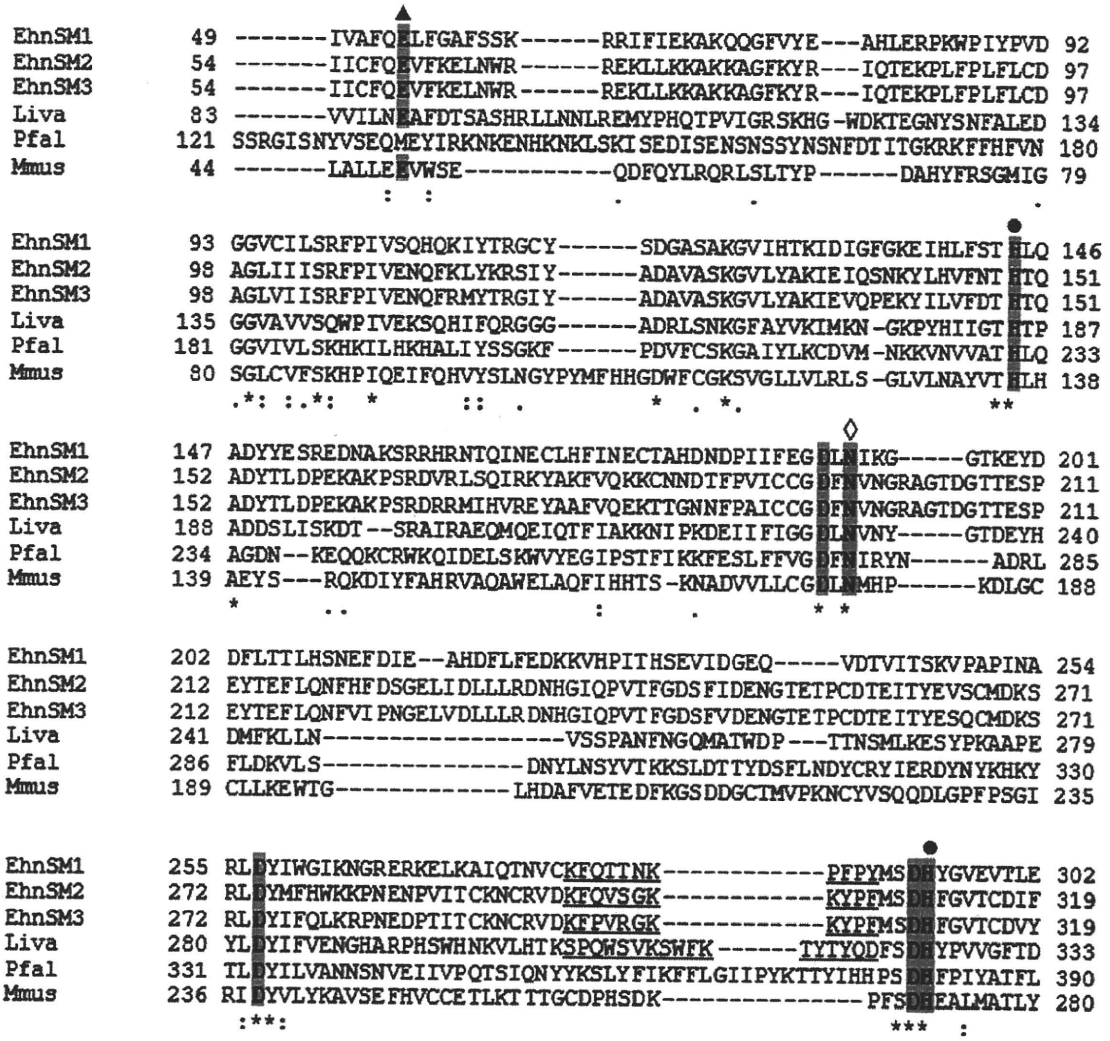

Fig. 1. Sequence alignment of *E. histolytica* neutral SMases. nSMases aminoacid sequences from *Listeria ivanovii* (Liva), *Plasmodium falciparum* (Pfal) and *Mus musculus* (Mmus) are aligned with EhnSM1, EhnSM2 and EhnSM3 from *E. histolytica*. The residues with 100% conservation in all sequences are indicated by asterisks, and those important for the catalysis are highlighted in grey. The Mg^{2+}-complexing glutamic acid (▲), the asparagines involved in substrate binding (◊), and the two histidine residues that act as the general base and acid (●) are remarked. β-Hairpin is italicized. The alignment was produced using CLUSTAL W (Thompson et al., 1994).

desalting column (Amersham Pharmacia Biotech) and eluted with 100 mM Tris–HCl, 20 mM NaCl pH 7.5. The activity of the purified rEhnSM1 was determined as previously described. For inhibition studies, the rEhnSM1 was preincubated with various concentrations of scyphostatin for 30 min at 4 °C before addition of the substrate. Scyphostatin was a generous gift from, Sankyo Co., Ltd., Tokyo, Japan.

2.7. Production of *E. histolytica* transfectants overexpressing *EhnSMases*

The EhnSM1 and EhnSM3 protein coding region was amplified by PCR from cDNA using sense and antisense oligonucleotides containing appropriate restriction sites. For EhnSM1 coding region (EHI_007460) amplification, sense primer 5′-TCCCCCGGGATGAACA ATCCCCTT-3′ and antisense primer 5′-CCG*CTCGAG*TTACAATAATTC TAG-3′; for EhnSM3 (EHI_125790) sense primer 5′-TCCCCCGGGATG GCAGAAGAAGCC-3′ and antisense primer 5′-CCG*CTCGAG*TTAAAG ATAAACGTC-3′ (restrictions sites are italicized). A sequence tag consisting of three tandem repeats of hemagglutinin (HA) peptide was inserted at the amino terminus. A PCR-amplified DNA fragment was digested with *Sma*I and *Xho*I, and ligated into corresponding sites of the expression vector pEhEx (Saito-Nakano et al., 2004), to produce phex-nSM1 and phex-nSM3. The wild-type trophozoites were transformed with either phex-nSM1, phex-nSM3 or pEhEx by liposome-mediated transfection as previously described (Nozaki et al., 1999).

2.8. Indirect immunofluorescence microscopy

Ameba transformants in exponential growth were harvested and transferred to 8 mm round wells on glass slides, fixed with 3.7% paraformaldehyde, and permeabilized with 0.2% saponin/1% BSA/PBS as previously described (Saito-Nakano et al., 2004). The cells were then reacted with anti-HA 16B12 mouse monoclonal antibody (1:1000) (Berkeley Antibody Co.) and Alexa Fluor-568, anti-mouse secondary antibody (1:1000) (Molecular Probes). For the staining of lysosomal compartments, amebas were pulsed with LysoTracker™ Red DND-99 (Molecular Probes) (1:500) for 12 h at 35 °C. Samples were examined on a Carl-Zeiss LSM510 confocal laser-scanning microscope (Thornwood, NY). Images were further analyzed using LSM510 software.

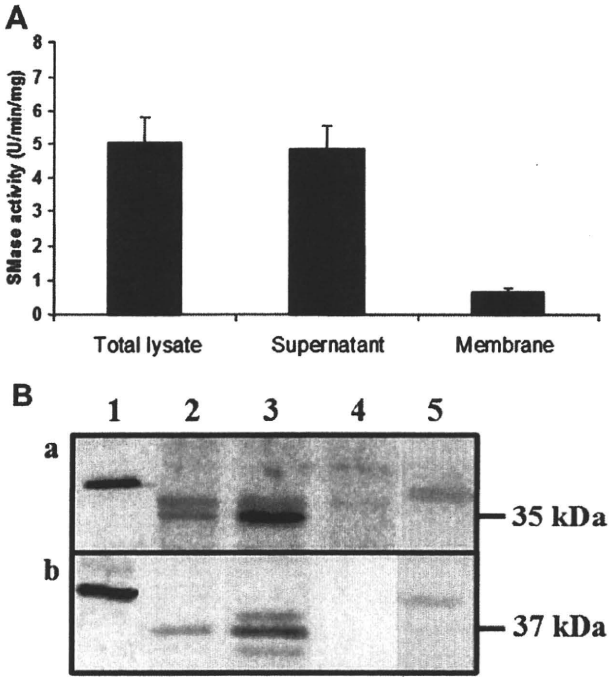

Fig. 2. nSMase activity and western blot analysis of SMases in *E. histolytica* cellular fractions. (A) After lysis of the harvested trophozoites by mechanical disruption, the supernatant and membranal fractions were separated as described in Section 2. Each fraction was assayed for nSMase activity at pH 7.5. The values of specific activity of nSMase are the mean of triplicate experiments. (B) Recombinant EhnSM1 and EhnSM3 as well as cellular fractions of *E. histolytica* were subject to SDS–PAGE, transferred to nitrocellulose, and reacted with corresponding polyclonal antibodies anti-EhnSM1 (a, lanes 1–4), anti-EhnSM3 (b, lanes 1–4) or anti-HA (a and b, lane 5). Horseradish peroxidase-conjugated anti-rabbit goat serum was used as secondary antibody. Purified recombinant protein EhnSM1 (lane 1a) and EhnSM3 (lane 1b); total lysate (lane 2); supernatant fraction (lane 3); membranal fraction (lane 4). Total lysate of *E. histolytica* transformants overexpressing HA-epitope tagged EhnSM1 (lane 5a) and EhnSM3 (lane 5b).

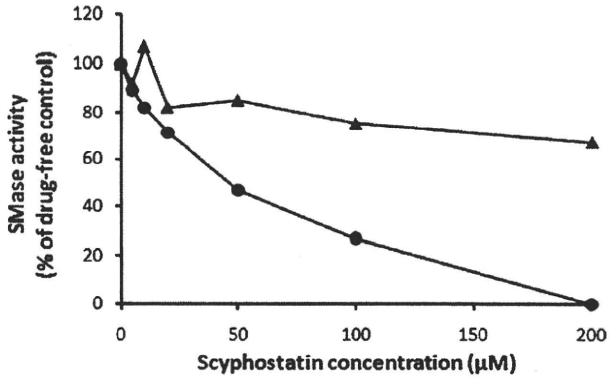

Fig. 3. Effect of scyphostatin on nSMase activity from *E. histolytica*. Recombinant EhnSM1 protein and bacterial SMase from *B. cereus* were incubated with various concentrations of scyphostatin for 30 min on ice. SMase activity of amebic (circles) and bacterial enzyme (triangles) were determined in the presence of 0.5 mM of Mn^{2+}, as described in Section 2. The activity is shown as percentage of control activity determined in the absence of the drug.

3. Results

3.1. Sequence analysis of genes encoding putative neutral SMases in E. histolytica

A search for annotated sequences encoding SMases was done in the genome of *E. histolytica* (Loftus et al., 2005; http://www.tigr.org/tdb/e2k1/eha1). Three genes were found encoding putative neutral sphingomyelin phosphodiesterases: *Ehnsm1* (EHI_007460), *Ehnsm2* (EHI_178990), and *Ehnsm3* (EHI_125790). Other five sequences are annotated (EHI_103250, EHI_022610, EHI_193190, EHI_067710, EHI_088080), that are identical to *Ehnsm1* including the promoter region (data no shown). Amebic putative nSMases *Ehnsm2* and *Ehnsm3* are closely related sharing 87% and 89% of identity at nucleotide and amino acid level, respectively. They have 56–57% of identity at nucleotide level, and 36% at amino acid level with *Ehnsm1*. Similarities are restricted to catalytic motifs suggesting that those genes encode functional nSMases in *E. histolytica*. Residues important for the catalysis, asparagines involved in substrate binding, Mg^{2+}-complexing glutamic acid, and two histidine residues that act as the general base and acid, are conserved in the amebic sequences encoding nSMases (Fig. 1), suggesting that these putative nSMases are active. RT-PCR experiments using specific primers showed that all the putative nSMase genes are actively transcribed. In addition, microarrays data showed *Ehnsm1* as the highest expressed gene, followed by *Ehnsm3* and *Ehnsm2* (data not shown).

3.2. Activity of SMase in E. histolytica and effect of bivalent ions

To determine whether *E. histolytica* possesses nSMase activity, exogenous SM hydrolysis was measured at pH 7.5 in amebic total lysates, membranal and soluble fractions (Fig. 2A). A commercial preparation of purified nSMase from *B. cereus* was included as a control (data not shown). Approximately 95% of the *E. histolytica* nSMase activity was found in the soluble fraction (Fig. 2A). It has been reported that Mg^{2+} and Mn^{2+} ions enhance the activity of nSMases, while Zn^{2+} and Cu^{2+} inhibit it (Clarke and Hannun, 2006). nSMase activity from the soluble fraction of *E. histolytica* was evaluated in the presence of different concentrations of bivalent ions such as Mg^{2+}, Mn^{2+}, Ca^{2+} and Zn^{2+}. Mg^{2+} or Ca^{2+} had no significant effect on the activity, 2 mM Zn^{2+} reduced the activity to 50% whereas 0.5 mM Mn^{2+} stimulated the activity 3-fold (Table 1). The presence of chelating agents such as EDTA or EGTA in the reaction mixture had no effect on the basal activity.

Table 1
Effect of bivalent ions on nSMase activity of *E. histolytica* and recombinant EhnSM1 purified from *E. coli*.

mM	Supernatant fraction from *E. histolytica*					Recombinant EhnSM1		
	Mg^{2+}	Mn^{2+}	Ca^{2+}	Zn^{2+}	EGTA	Mn^{2+}	Zn^{2+}	EGTA
nSMase activity (% of control)[*]								
0	100	100	100	100	100	100	100	100
0.25	104	289	99	82	–	–	–	–
0.5	107	285	110	79	–	450	–	–
1	94	258	99	74	–	–	–	–
5	103	227	101	52	95	–	12	97

[*] The activity is shown as relative values of the control activity determined in the absence of the cations.
– No determined.

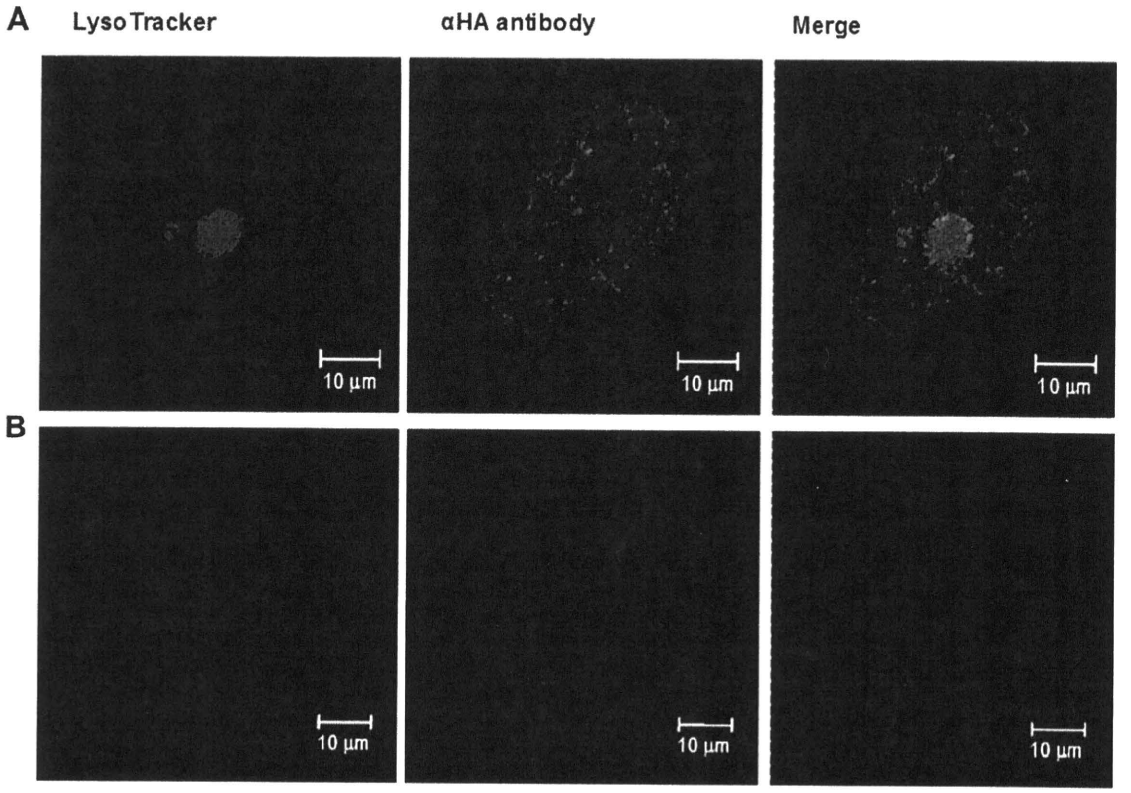

Fig. 4. Subcellular localization of EhnSM1 and EhnSM3 in *E. histolytica* trophozoites. Subcellular localization of EhnSM1 and EhnSM3 was examinated by immunoflueresce assay using ameba transformants overexpressing HA-tagged EhnSM1 (A) and HA-tagged EhnSM3 (B). Amebae were pulsed with LysoTracker Red, a membrane diffusible probe accumulated in acidic organelles (and then subject to immunofluorescence assay with anti-HA antibody. Localization of HA-tagged proteins (green) and LysoTracker (red) is shown. (For interpretation of the references to colour in this figure legend, the reader is referred to the web version of this article.)

3.3. Characterization of recombinant EhnSM1 produced in E. coli

To determine if *Ehnsm1–3* encode functional nSMases, a representative amebic nSMase, EhnSM1, was expressed as recombinant protein linked to a histidine tag in *E. coli*. The nSMase activity was found for the purified product (Table 1). The activity of the recombinant EhnSM1 increased 4.5-fold in the presence of 0.5 mM Mn^{2+}, and it was inhibited by 5 mM Zn^{2+}, as it was shown for the nSMase activity in the amebic supernatant fraction. Chelating agents had no effect on the recombinant protein activity (Table 1). Phosphatidylserine (PS), a phospholipid that has been reported to stimulate nSMases (Hanada et al., 2000), had no effect on rEhnSM1 (data not shown). Scyphostatin, a potent and specific inhibitor of mammalian nSMases but not aSMases (Nara et al., 1999), shows a dose-dependent inhibition of SMase activity of recombinant EhnSM1 with a complete abolition of activity at 200 μM, showing an IC_{50} of 43 ± 9 μM. The SMase from *B. cereus* was only partially inhibited (30%) by 200 μM scyphostatin (Fig. 3) Previous studies reported that bacterial SMases are only affected with concentrations above 1 mM (Nara et al., 1999).

3.4. Immunodetection of SMases in the soluble fraction of E. histolytica

Ehnsm1 encodes an enzyme of 35 kDa with a pI of 6.4, and *Ehnsm2* and *Ehnsm3* encode 37 kDa enzymes with pI of 7.9 and 6.1, respectively. Predictions by PSORT (Nakai and Kanehisa, 1992) and Signal P (Nielsen et al., 1997), suggest that all of them are cytoplasmic. The presence of nSMases in the trophozoites was evaluated by western blot using polyclonal antibodies raised against recombinant EhnSM1 and EhnSM3. These antibodies predominantly detected 35 and 37 kDa proteins, respectively, corresponding to the predicted molecular weight in the total homogenate and soluble fraction (Fig. 2B). Additional bands were only weakly detected, probably representing cross-reaction with the other nSMases. No signal was detected associated to the membranal fraction. Purified recombinant protein EhnSM1 and EhnSM3 were used as control.

3.5. Subcellular localization of SMases in E. histolytica

Amebic transformants expressing HA-tagged EhnSM1, EhnSM2, and EhnSM3 were created to examine the localization of individual EhnSM isotypes. The expression of the HA-tagged SMases was confirmed by western blot analysis (Fig. 2). The bands detected correspond to the predicted molecular weight for each HA-tagged SMase. Immunofluorescence imaging using anti-HA antibody showed that EhnSM1 and EhnSM3 are distributed to the cytosol without a co-localization with lysosomes (Fig. 4). Transfectants expressing HA-tagged EhnSM2 also showed cytosolic distribution (data not shown).

4. Discussion

In the present work, we characterized the nSMase activity that is present in this parasite and we showed the evidence of *Ehnsm1* gene functionality. *In silico* analysis revealed three genes encoding putative nSMases annotated in the *E. histolytica* genome. In humans, nSMases are encoded by three genes showing differential tissue-associated mRNA expression pattern. Their products observe differences of substrate specificity and cation-dependence, and are differentially stress-regulated (Krut et al., 2006; Corcoran et al., 2008). Genes encoding nSMases in *E. histolytica*, show differences at their expression level in basal conditions. Previously, *E.*

histolytica microarray data, showed an up-regulation for *Ehnsm1* due to heat shock stress (MacFarlane and Singh, 2006). An *Ehnsm* down-regulation was observed in monoxenic cultures of *E. histolytica* with *E. coli* O55 (Mendoza-Macías et al., 2009). These results suggest a differential regulation of EhnSMase genes.

Predicted amino acid sequences of amebic nSMases show low homology to prokaryotic and eukaryotic nSMases reported to date; however they share conserved catalytic aminoacid residues, suggesting that the neutral SMase activity in *E. histolytica* correspond to the genes coding nSMases. Human nSMase1 and nSMase2 show no apparent homology with nSMase3, however nSM2 and nSM3 displayed similar biochemical properties (Krut et al., 2006). *B. cereus* nSMase, a bacterial protein used as a model in structural analysis of nSMase catalysis, shows 20% of homology with mammalian nSMases (Ago et al., 2006). Despite this low similarity reported between nSMases sequences from different organisms, important residues involved in catalytic activity are conserved, indicating a similar mechanism. In this context, is not surprising that amebic nSMase sequences show low homology with other previously reported nSMases.

The predicted molecular mass for the amebic nSMases of 35–37 kDa was confirmed by western blot. This molecular mass is similar to those from prokaryotic organisms such as *L. ivanovii* (38.5 kDa) (González-Zorn et al., 1999), *B. cereus* (36.9 kDa) (Yamada et al., 1988) and *S. aureus* (37.4 kDa) (Sueyoshi et al., 2002); meanwhile eukaryotic nSMases show higher molecular mass such as in *P. falciparum* (46 kDa) and human (47.6, 60 and 97.8 kDa) (Hanada et al., 2002; Krut et al., 2006). Although the enzymes from prokaryotic and eukaryotic organisms share some biochemical properties *in vitro*, each one has different biological function. The biological role of the novel *E. histolytica* nSMases described in this work remains to be determined.

In silico analysis of *E. histolytica* nSMase genes suggested a cytosolic localization, which was confirmed by enzymatic activity assays and immunodetection on cellular fractions of *E. histolytica*. This was further supported by immunolocalization of overexpressed HA-epitope tagged nSMases in the amebic trophozoites. All the evidences indicate that amebic nSMases are cytosolic proteins. One question that arises about soluble amebic nSMases, is regarding the interaction of these enzymes with sphingomyelin, which is mostly localized at the outer leaflet of plasma membrane. nSMases from other eukaryotes have either N- or C-terminal extensions that encode predicted membrane-spanning regions, which localize these proteins to membranes and promote interfacial catalysis. In contrast, bacterial SMases, encoded by one gene, lack any obvious membrane-spanning regions and are secreted (Openshaw et al., 2005). None of the predicted amebic nSMases contains an obvious membrane interaction motif. Analysis of the crystal structure of the *L. ivanovii* and *B. cereus* SMases, both non-membranal proteins, revealed a unique hydrophobic beta-hairpin region located at the C-terminus that protrudes into the solvent with the two aromatic amino acid residues that are important for the interaction of these enzymes with the membrane (Openshaw et al., 2005; Ago et al., 2006). From the sequence alignment as well as tertiary structure prediction (data not shown), the beta-hairpin region is conserved in all amebic nSMases, suggesting a similar mechanism of potential membrane interaction. Although IFA did not show any evidence of membrane association, a temporal recruitment after specific stimuli is not discarded.

Amebic nSMases show low homology with other nSMases, however EhnSM1 shared biochemical properties. Cation effect results indicate that nSMase activity in the cytosolic fraction is Mg^{2+}-independent, stimulated by Mn^{2+} and inhibited by Zn^{2+}. The same properties were found in the recombinant EhnSM1 protein purified from *E. coli*. However, the native nSMase and the recombinant have different sensitivity to the Mn^{2+} and Zn^{2+}. Probably the native activity determined in the supernatant fraction of *E. histolytica* is the contribution of several nSMases and each one could have different cation sensitivity. These properties resemble the mammalian cytosolic Mg^{2+}-independent nSMase (Okazaki et al., 1994), and some bacterial SMases (Sueyoshi et al., 2002). *P. falciparum* and mammalian cells also have a membrane-associated Mg^{2+}-dependent nSMases that apparently are not present in *E. histolytica*. In addition, amebic nSMase activity is not stimulated by PS *in vitro* as *B. cereus* SMase (data not shown), in contrast to mammalian nSMase activity which is enhanced by this anionic phospholipid (Liu et al., 1998). Amebic nSMase1 is sensitive to inhibition by scyphostatin, a specific nSMases inhibitor; its value of IC_{50} is higher compared with values observed for *P. falciparum* and bovine brain nSMases (Hanada et al., 2000).

Recently, sphingolipids, in particular ceramide, have emerged as important lipid second messengers. Ceramide has been associated with cellular responses to stress, cell growth differentiation, and apoptosis in various eukaryotes including mammals and yeasts (reviewed by Clarke and Hannun, 2006). The SMases have been implicated in a major pathway of stress-induced ceramide-production, where the mammalian lysosomal acidic SMase and the Mg^{2+}-dependent neutral SMase are involved. nSMase activity was induced by a variety of stimuli such as cytokines, cellular stresses such as UV light, ROS, chemotherapeutic drugs, and pathological stimuli for example amyloid-β peptides and lipopolysaccharide (Levade and Jaffrézou, 1999; Marchesini and Hannun, 2004; Castillo et al., 2007). An increase in this activity was reported following treatment with DNA-damaging drugs and after treatment of epithelial lung cells with RNS (Castillo et al., 2007). It was found recently that nSMase3 gene expression is regulated by DNA damage and nongenotoxic stress, and that it is deregulated in human malignancies (Corcoran et al., 2008). By analogy, nSMases could be involved in the production of ceramide associated with stress responses in this parasite. Recently an apoptosis phenomenon has been observed in *E. histolytica* cultured in the presence of G418, an analogue of neomycin (Villalba et al., 2007). However the mechanism involved in the parasite remains unclear.

In *G. lamblia*, the genes *gsmase B* and *gsmase 3b* are upregulated during encystation suggesting that scavenging ceramide from dietary components present in the small intestine is an important feature for encystation of this parasite (Hernandez et al., 2008). The bacterial SMases cause hemolysis and are thus a potential virulence factors such as the *S. aureus* SMase, also known as a β-toxin (Bramley et al., 1989; Sueyoshi et al., 2002). Several microorganisms producing SMases are usually serious or opportunistic pathogens. Although the relationship between microbial SMase and infectious disease is still unclear at the molecular level, SMase could cause hemolysis when SMase-producing microbes invade the host. Hemolytic activity has been reported in *E. histolytica* (López-Revilla and Said-Fernández, 1980) and two *E. histolytica* phospholipases have been associated with this activity. It has been proposed that heat-stable factors, such as free-fatty acids contribute with the hemolytic activity (Long-Krug et al. 1985; Said-Fernández and López-Revilla, 1988), but the complete nature of this activity is unknown. Obvious secretion motif was not found in any of the annotated sequences for amebic nSMases. Further characterization of nSMase activity in *E. histolytica* is necessary to know its role in virulence as well as in cell signaling. Ongoing studies employing EhnSM gene silenced strains might help to define the function of these enzymes in the parasite.

Acknowledgments

We thank I. Páramo-Pérez and A. Rangel-Serrano for their technical assistance. This investigation was supported by the Grants C01-41702/A-1 from CONACYT and the research institutional sup-